

ELECTROMIGRATION IN MACROSCOPIC RELAXATION OF STEPPED SURFACES*

JOHN QUAH[†] AND DIONISIOS MARGETIS[‡]

Abstract. We study the effect of an external electric field \mathbf{E} on macroscopic relaxation laws for crystal surfaces in $2 + 1$ dimensions. We derive a nonlinear, fourth-order partial differential equation (PDE) for the surface height from the microscale motion of line defects (steps). This PDE contains a linear-in- \mathbf{E} convective contribution and reflects a variety of microscale kinetic processes. A basic ingredient is an extended Fick’s law for the surface flux, which accounts for drift of adsorbed atoms (adatoms), isotropic as well as anisotropic diffusion of adatoms on terraces between steps, attachment-detachment of atoms at step edges, edge atom diffusion, and atom desorption into the surrounding vapor. In particular, we discuss conditions that enable the neglect of desorption. By resorting to stationary PDE solutions, we show how \mathbf{E} can possibly influence spatial changes of the slope profile near a macroscopically planar surface region (facet). We start with the Burton–Cabrera–Frank model for the motion of interacting steps, which is viewed as a discrete scheme for the macroscopic description, and apply coarse graining by separating local space variables into fast and slow.

Key words. epitaxial relaxation, crystal facet, Burton–Cabrera–Frank model, electromigration, desorption, surface diffusion, step chemical potential, macroscopic limit, variational principle

AMS subject classifications. 35Q99, 35R35, 74A50

DOI. 10.1137/090760635

1. Introduction. Patterns on crystal surfaces figure prominently in the fabrication of novel optoelectronic devices. The stability of nanoscale surface features has attracted much interest in recent decades, for example, in the context of mobile communications technology [48]. Emerging issues concern the control of surface morphological evolution, e.g., by varying temperature, elastic stress, material deposition from above, or the effect of an external electric field on charged surface atoms (“electromigration”). In particular, electromigration plays a crucial role in the degradation or failure of connections in microelectronics [14].

Crystal surface evolution is driven by the diffusion of adsorbed atoms (adatoms) on nanoscale terraces, along with other microscale kinetic processes such as desorption of atoms from the surrounding vapor, and atom attachment-detachment at line defects (steps). These mechanisms are intrinsic to crystals. The theoretical underpinnings of step motion were set forth by Stranski [52] and Burton, Cabrera, and Frank (BCF) [2].

External effects such as an electric field [14] are introduced experimentally to *control* surface patterns [16, 30]. The field can accelerate the rate of thermal decay of surface morphologies. Related experimental data are used to estimate the effective charge of adatoms [13]. The electric current causes a *bias* in the diffusion of adatoms:

*Received by the editors May 30, 2009; accepted for publication (in revised form) November 30, 2009; published electronically February 19, 2010.

<http://www.siam.org/journals/mms/8-2/76063.html>

[†]Department of Mathematics, University of Maryland, College Park, MD 20742-4015 (jquah@math.umd.edu). This author’s research at the University of Maryland was supported by a Monroe Martin Graduate Fellowship during the summer of 2008 and by NSF-MRSEC DMR0520471 during the spring of 2009.

[‡]Department of Mathematics, and Institute for Physical Science and Technology, and Center for Scientific Computation and Mathematical Modeling, University of Maryland, College Park, MD 20742-4015 (dio@math.umd.edu). This author’s research was supported in part by NSF-MRSEC DMR0520471 and by NSF DMS0847587 at the University of Maryland.

at long times, the adatoms tend to move along the applied current. This effect coexists with processes captured by an *anisotropic* adatom mobility at the macroscale [28].

In this article, we extend previous macroscopic descriptions of crystal surface dynamics [26, 28, 39] to incorporate the effect of an electric field into a partial differential equation (PDE) for the surface height in $2 + 1$ dimensions. In our approach, the PDE *emerges* as the limit of a discrete scheme for step flow and incorporates a rich variety of kinetic processes (drift, desorption, and terrace anisotropy). We study how the applied field influences the slope profile, especially near a macroscopically flat surface region (facet). We focus on relaxation, when surfaces evolve toward planarity by lowering their free energy. The resulting PDE combines (i) a kinetic anisotropy with a *drift velocity* for the adatom flux, and (ii) a variational principle for a thermodynamic force, the step chemical potential. The PDE is in principle not valid across surface peaks and valleys [28].

Our intention with this work is twofold. First, we aim to clarify the limiting procedure by which the BCF model is coarse-grained in the presence of joint physical effects, e.g., desorption and electromigration, for monotonic step trains. Second, we seek to gain analytical insight into how the electric field (which affects a PDE coefficient) can possibly influence the slope profile near a facet. For this purpose, we use stationary solutions and assume that the slope profile approaches zero near the facet edge.

This work is motivated by the need to describe systematically how microscopic parameters for surface kinetics are related to the macroscopic decay of the height profile in electromigration. Features of this decay are experimentally measurable [13].

We start with a microscopic model that incorporates an electric field into the BCF theory and has been widely established in theoretical treatments of electromigration; see, e.g., [3, 4, 12, 13, 14, 17, 18, 19, 20, 21, 22, 29, 31, 34, 36, 37, 42, 43, 44, 49, 50, 57, 58]. These previous works focus on the development of instabilities (e.g., step meandering and bunching) across scales, often from a dynamical system viewpoint. We, on the other hand, place electromigration in the context of connecting discrete schemes for interacting steps to global PDE laws and variational principles in $2 + 1$ dimensions [5, 26, 28, 32, 33, 39, 41, 46, 47, 56]. Our work is an extension of previous two-dimensional (2D) laws [28, 39]. Numerics for the PDE with an electric field and negligible step line tension (without facets) are presented elsewhere [1].

The starting point of our analysis consists of coupled differential equations for step positions. The macroscopic PDE is sought for a coarser scale, in the limit of zero step size. This description has compelling advantages, involving only one dependent variable, the surface height. (By contrast, at the BCF level many steps are tracked.)

There is a vast body of literature in epitaxial phenomena. For broad reviews on this subject, the reader may consult, e.g., [8, 16, 18, 30, 35].

1.1. Microscale motion. Generally speaking, there are three distinct scales for crystal surfaces: atomistic scale, nanoscale, and macroscale. The atomistic approach in principle seeks solutions to many-body equations for electrons and nuclei or suitably defined atoms over relatively short time and length scales [54]. This description, although vital to obtaining material parameters, is not of our concern here.

At the nanoscale, below the roughening transition temperature [16], crystal surfaces have distinct steps and terraces and can develop facets. According to the BCF model [2], step edges move by mass conservation in response to the following: (i) atom attachment and detachment at step edges; and (ii) diffusion of adatoms on terraces. Additional kinetic effects are atom desorption and edge atom diffusion. Furthermore,

the step edge curvature (or stiffness) and step entropic and elastic dipole interactions [23] contribute to a thermodynamic driving force, the step chemical potential. In this perspective, the aggregate adatom motion on each terrace is approximated by a continuous adatom density. This density satisfies a diffusion equation for which the step edges are continuous moving boundaries.

1.2. Electromigration and desorption at BCF level. An externally applied (vector-valued) electric field, \mathbf{E} , tends to force adatoms to move in its direction, causing a drift velocity \mathbf{v} . This \mathbf{v} is related to \mathbf{E} by [4, 13]

$$(1.1) \quad \mathbf{v} = \frac{D_s(Z^*e)\mathbf{E}}{T},$$

where D_s is the adatom diffusivity, Z^*e is the effective adatom charge,¹ and T is the temperature (or, Boltzmann energy $k_B T$ in units where $k_B = 1$). At the level of steps, the electric field amounts to the addition of a convective (linear in the density gradient) term in the diffusion equation for the adatom density; see (3.2). Regarding (1.1), $|Z^*|$ is larger than unity for metals but can be much smaller than unity for semiconductors [4]. This Z^* has been estimated in experiments via comparisons of data for decay rates with predictions of the microscopic model; see, e.g., [13]. Note that \mathbf{E} influences the temperature in an experimental setup, since it directly controls the electric current that flows through and eventually heats up the sample.

Theoretical works in electromigration appear to have initially been motivated by experimental observations of different stability regimes of vicinal Si(111) surfaces [20].² Related proposals (although not directly relevant to our focus here) include but are not limited to the early work by Stoyanov [49] and more recent investigations by Pierre-Louis and Métois [34, 37], and by Zhao, Weeks, and Kandel [57, 58].

In addition to electromigration, we will allow adatoms to desorb into the vapor with characteristic time τ . So, the term C/τ is added in the adatom diffusion equation where C is the adatom density. We study if and how this addition at the BCF level influences the macroscopic limit. Note that a phenomenological approach to desorption in crystal morphological evolution is offered by Villain [55]. We derive τ -dependent corrections of the large-scale flux and describe how large τ needs to be so that desorption can be neglected in the macroscopic laws. In addition, we enrich the microscale model with other kinetic processes, namely, *anisotropic* terrace diffusion and *edge atom* diffusion.

1.3. Macroscopic limit and assumptions. The macroscopic limit aims to describe a continuous surface at sufficiently large scales. Previous studies of electromigration and desorption apparently have not focused on global evolution laws for the surface height, and hence carry a perspective different from ours. These works (i) focus mainly on stability issues, (ii) make use primarily of nanoscale models where steps are everywhere parallel, and (iii) allow steps to interact mainly through terrace diffusion (with less emphasis on step-step entropic or elastic dipole interactions).

Our derivation uses the multiscale expansion introduced in [28], which is essentially not limited by the $(2 + 1)$ -dimensional geometry. The expansion parameter is the step height a . This formulation relies on the separation of local variables for interacting steps into fast and slow, and can encompass additional physical effects such

¹Here, we follow the notation of [4]. The symbol Z^* (with an asterisk) should not be confused with the usual symbol for the conjugate of a complex number.

²The index (111) indicates the direction of the normal vector, i.e., the surface orientation with respect to the high-symmetry (x, y) plane.

as desorption and electromigration. As a result, we derive a fully continuum model in 2 + 1 dimensions that is more general than the model developed in [28]. The additional effect of anisotropic terrace diffusion is also incorporated subsequently, offering an extension of a previous theory [39].

The (geometric in nature) assumptions underlying the macroscopic limit are worth stressing [28]. We require that the (microscale) terrace width is of the order of the step height a and small compared to the following: (i) the step radius of curvature; (ii) the length over which the step curvature varies; and (iii) the macroscopic length over which the step density varies. A step train satisfying these conditions is referred to as “slowly varying” [28]. The step height a is the *smallest possible length in this setting*. The full continuum limit is reached formally as $a/\lambda \downarrow 0$ where λ is a macroscopic length. The step density is fixed and approaches the surface slope. We assume that the initial (at $t = 0$) ordering of steps is preserved by the flow (for $t > 0$),³ and that step trains are *monotonic*, say, with descending steps in the direction of increasing coordinate.

Furthermore, we require that certain kinetic parameter groups involving the step height a remain $\mathcal{O}(1)$ (as $a/\lambda \downarrow 0$). In particular, we take $D_s/(ka) = \mathcal{O}(1)$ where k is any relevant kinetic rate for attachment-detachment of adatoms at a step edge.

1.4. Main results. The central result of our work is an extension of Fick’s law expressing the vector-valued flux \mathbf{J} for diffusion and drift of adatoms at large scales:

$$(1.2) \quad \mathbf{J} = -C_s e^{\mu/T} \mathbf{M} \cdot \left(\nabla \mu - \mathbf{v} \frac{T}{D_s} \right),$$

where \mathbf{M} is an effective mobility, in principle a second-rank tensor given by (4.4) for isotropic terrace diffusion [28, 39], μ is the macroscale step chemical potential, and C_s is the equilibrium density of adatoms at a straight step edge; see section 5.1. In the case with $|\mu| \ll T$, (1.2) becomes

$$(1.3) \quad \mathbf{J} = -C_s \mathbf{M} \cdot \left[\nabla \mu - \mathbf{v} \frac{T}{D_s} \left(1 + \frac{\mu}{T} \right) \right];$$

see Proposition 4.1. Because of the relative simplicity of the derivation and the wide applicability of the linearization with μ [16], (1.3) is derived first while (1.2) is provided as an extension. Equations (1.2) and (1.3) rely on an approximate solution to the 2D adatom diffusion equation; see Proposition 3.1. An assumed condition is $|\mathbf{v}| \ll k$ where k is a typical kinetic rate of atom attachment-detachment at a step; see Remark 3.2. This condition implies that the adatom drift is slow relative to atom attachment-detachment at step edges and is met in physical situations; see, e.g., [4, 13].

Various forms of the tensor mobility \mathbf{M} have been derived. Extensions of (1.2) and (1.3) to desorption and anisotropic terrace diffusion are described in sections 5.2 and 5.3, paving the way to a reasonably general macroscopic theory of surface relaxation.

For entropic and elastic dipole step interactions, the μ entering (1.3) is the variational derivative of the surface free energy (see, e.g., [26, 28] and references therein)

$$(1.4) \quad E[h] = \int dA \gamma(x, y), \quad \gamma = g_1 |\nabla h| + (g_3/3) |\nabla h|^3,$$

where g_1 is proportional to the step line tension, g_3 is the step-step interaction strength, and $dA = dx dy$; see (4.2). (Note that the energy density γ is singular

³This property should be derivable from microscale dynamics. This aspect is not studied here.

at $\nabla h = 0$.) In this model, surface regions defined as $\mathcal{F}_t = \{(x, y, h) \in \mathbb{R}^3 \mid \nabla h = 0\}$ correspond to facets, i.e., macroscopic plateaus (of spatially constant height). By complementing (1.2) or (1.3) and μ with the adatom mass conservation law (4.1), we obtain a PDE for h ; see (4.16) with (4.14) and (4.15) under $|\mu| \ll T$. This PDE is not applicable across \mathcal{F}_t .

Connections of the macroscopic PDE with documented step instabilities under an electric field are discussed for one-dimensional (1D) geometries. Such instabilities arise from backward-diffusion terms in the PDE; see section 6.1. Straight- and circular-step morphologies are considered here. In particular, the radial case (with a radial drift) has not been studied experimentally and thus appears less tangible practically. However, there is no physical principle that prohibits having a radial setting with drift. We adopt the view that our radial model may illustrate the interplay of step curvature and drift in physical situations (where steps are curved). Our analysis indicates that a step-up drift can be tuned to balance the destabilizing effect of step curvature (line tension).

With regard to facets, as is known from 1D geometries [26, 27], it is assumed herein that the positive surface slope, $m(\mathbf{r}, t) = |\nabla h|$, exhibits the behavior $m = \mathcal{O}(d_\perp^{1/2})$ for sufficiently small d_\perp , under slope continuity; d_\perp is the distance from a point of the sloping surface to the facet boundary along its normal. In section 6.2, we discuss how this behavior can possibly be manipulated by an electric field, by drawing examples from the straight-step and radial cases with diffusion limited kinetics for stationary PDE solutions. Interestingly, m tends to increase by a large enough drift velocity in the step-down direction, but recovers its square-root behavior for a drift in the step-up direction. Our analysis invokes slope continuity and (1.3) in a time-independent setting, thus avoiding the (as yet unresolved) issue of boundary conditions near a moving facet [27].

1.5. Limitations. We assume that steps move near thermodynamic equilibrium, which is fairly reasonable for surface relaxation (in the absence of growth). We do not make any effort to further justify the applicability of BCF theory [2], which is invoked here. A macroscale theory under far-from-equilibrium conditions may still be possible, but is not of our concern in this work.

Because of the step train monotonicity that we impose, our limiting procedure is not strictly valid across (non-faceted or faceted) surface peaks and valleys, where $\nabla h = 0$. An open question is how to carry out the macroscopic limit near these surface extrema. In the case with axisymmetric mounds having a facet, the continuum variational formulation of the PDE has been shown to be consistent with the step motion if the facet size becomes vanishingly small, which is the limit of zero step line tension [27]. In the presence of facets, however, solving the evolution equation constitutes an essentially unresolved free boundary problem [15, 27, 47].

We assume that any possible surface instabilities do not violate the assumptions for the full continuum limit. Previous studies of the microscopic dynamics for electromigration have shown that steps can bunch or meander [4, 12, 16, 21, 36, 42]. The macroscopic PDE here does capture the tendency of steps to bunch, as discussed in section 6.1. The fully continuum theory is, of course, applicable to regions where such instabilities do not perturb the geometry too far from a slowly varying step train.

Patterns on crystal surfaces are also created by material deposition from above, which adds a forcing in the adatom diffusion equation [38]. The deposition problem is not studied here. One reason is that the corresponding macroscale PDE in $2 + 1$ dimensions has a different character; the directions normal and parallel to step edges

induce distinct dynamics. This case is the subject of work in progress. Another reason is that the near-equilibrium character of the BCF model (which underlies the present treatment) may be of limited applicability in growth. Our assumption of no material deposition allows us to remove complications irrelevant to relaxation and isolate conveniently the effect of an applied electric field.

1.6. Article outline. The remainder of this article is organized as follows. In section 2, we review models of 1D steps. In section 3, we describe the geometry of a 2D step train and formulate the equations of motion with an electric field; in particular, we find explicit solutions for terrace diffusion. In section 4, we derive the macroscopic limit of step flow with drift in $2+1$ dimensions. In section 5, we propose extensions of the macroscopic theory, encompassing a nonlinear (exponential) law for equilibrium adatom density and step chemical potential, *desorption* of adatoms, and anisotropic terrace diffusion and edge atom diffusion. In section 6, we discuss two interrelated aspects of electromigration in 1D and possible extensions to 2D: in section 6.1, we revisit step bunching instabilities; and in section 6.2, we indicate how the electric field can influence the behavior of the slope profile near a facet edge. In section 7, we summarize our results and discuss open directions. Throughout this article, the terms “macroscopic limit,” “macroscale,” and “full continuum” are used interchangeably.

2. 1D microscale (step) models. In this section, we review briefly ingredients of step motion, including *repulsive* entropic and elastic dipole step interactions, for 1D geometries: straight and concentric circular steps. Related versions of the adatom diffusion equation with an electric field or desorption are solved explicitly.

The step configuration is shown in Figure 2.1. Both the diffusion of adatoms (density gradient) and electric field (drift velocity) contribute to the flux in each terrace. Each step advances or retreats in response to the net (normal) flux from the neighboring terraces. The surface evolves as the steps move, lowering its free energy.

2.1. Straight steps. The position of the i th step is denoted by $x_i(t)$ (t is time), where $x_{i+1} > x_i$ for all t , and $C_i(x, t)$ is the adatom density on the i th terrace, i.e., the region $x_i < x < x_{i+1}$. A *constant* electric field is applied externally in the x direction (perpendicular to steps), introducing a drift velocity v according to (1.1). The diffusion equation satisfied by $C_i(x, t)$ is

$$(2.1) \quad D_s \partial_x^2 C_i - v \partial_x C_i - \tau^{-1} C_i = \partial_t C_i \approx 0 \quad x_i < x < x_{i+1},$$

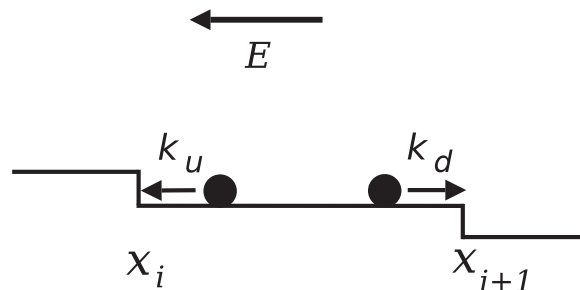


FIG. 2.1. Schematic of 1D steps (cross section) with an applied electric field E . Steps are descending with increasing x ; E is shown to be in the step-up direction ($E < 0$); and k_u (k_d) is the kinetic rate for atom attachment-detachment from a terrace to an up- (down-) step edge.

where τ is the characteristic desorption time; cf. (1) in [4]. We use the quasi-steady approximation, $\partial_t C_i \approx 0$, by assuming that step motion is much slower than diffusion. Equation (2.1) (particularly with $\tau = \infty$) is used widely in modeling electromigration [16], especially in determining the effective charge of adatoms [13].

The adatom flux on the i th terrace, $J_i(x, t)$, is defined by Fick’s law with drift [4]:

$$(2.2) \quad J_i(x, t) = -D_s \partial_x C_i + v C_i.$$

Linear kinetics prescribes the following boundary conditions at the step edges [16]:

$$(2.3a) \quad -J_i = k_u(C_i - C_i^{\text{eq}}) \quad x = x_i,$$

$$(2.3b) \quad J_i = k_d(C_i - C_{i+1}^{\text{eq}}) \quad x = x_{i+1};$$

k_u (k_d) is the kinetic rate for an up- (down-) step edge (accounting for an Ehrlich–Schwoebel barrier [6, 45]), and C_i^{eq} is the equilibrium adatom density at the i th step.

This C_i^{eq} expresses step interactions via the relation [16]

$$(2.4) \quad C_i^{\text{eq}} = C_s \exp\left(\frac{\mu_i}{T}\right) \sim C_s \left(1 + \frac{\mu_i}{T}\right), \quad |\mu_i| \ll T,$$

where μ_i is the i th-step chemical potential and C_s is the equilibrium adatom density at an isolated step. The linearization with μ_i is a common approximation in many theoretical treatments and works reasonably well in comparisons with experiments [16]. This simplification is relaxed in section 5.1. For *nearest-neighbor* step interactions,

$$(2.5) \quad \mu_i = \frac{\Omega g}{a} \frac{d}{dx_i} [V_{i,i+1} + V_{i,i-1}], \quad g > 0,$$

$$(2.6) \quad V_{i,i\pm 1} = \frac{1}{3} \left(\frac{a}{x_{i\pm 1} - x_i} \right)^2,$$

where $V_{i,j}$ describes the interaction between steps i and j , g (with units of energy) measures the magnitude of the step-step interaction energy, and Ω is the atomic area.

The velocity of the i th step is expressed via mass conservation,

$$(2.7) \quad \dot{x}_i = \frac{dx_i}{dt} = \frac{\Omega}{a} [J_{i-1}(x_i) - J_i(x_i)].$$

The system of equations for x_i that results from (2.1)–(2.7), together with the initial positions of steps, determine the subsequent evolution of the crystal surface.

To illustrate the model, we distinguish the cases (i) $\tau \rightarrow \infty$ (no desorption) and *nonzero* v , (ii) $v = 0$ with finite τ , and (iii) *nonzero* v and finite τ . For 2D, see section 5.2. The explicit time dependence is dropped (unless noted otherwise).

2.1.1. Electric field with no desorption. Solving (2.1) for $\tau \rightarrow \infty$ yields

$$(2.8) \quad C_i(x) = A_i e^{vx/D_s} + B_i \quad x_i < x < x_{i+1}.$$

The adatom flux on the i th terrace, $J_i(x)$, is computed by (2.2):

$$(2.9) \quad J_i(x) = v B_i.$$

Substituting for C_i and J_i in (2.3) via (2.8) and (2.9) leads to the system

$$(2.10) \quad \begin{pmatrix} e^{vx_i/D_s} & 1 + v/k_u \\ e^{vx_{i+1}/D_s} & 1 - v/k_d \end{pmatrix} \begin{pmatrix} A_i \\ B_i \end{pmatrix} = \begin{pmatrix} C_i^{\text{eq}} \\ C_{i+1}^{\text{eq}} \end{pmatrix}.$$

This matrix equation is solved explicitly to yield

$$(2.11) \quad J_i(x) = J_i(x_i) = -v \frac{C_{i+1}^{\text{eq}} - e^{v(\delta x_i)/D_s} C_i^{\text{eq}}}{e^{v(\delta x_i)/D_s}(1+v/k_u) - (1-v/k_d)},$$

where $\delta x_i := x_{i+1} - x_i = \mathcal{O}(a)$ is the terrace width. The step velocities, and thus the equations of motion for $x_i(t)$, are then obtained from (2.4)–(2.7).

In Appendix A we study the full continuum limit of (2.11) for the purpose of comparison with results of section 4; see (A.1). We find that, in the limit $\delta x_i \downarrow 0$ with fixed $a/\delta x_i$, (2.11) reduces to the 1D version of (1.3) with the mobility \mathbf{M} replaced by the scalar $(D_s/T)(1+q|\partial_x h|)^{-1}$, where $h(x)$ is the height profile, $q = 2D_s/(ka)$, and $k = 2(k_u^{-1} + k_d^{-1})^{-1}$. Here, we use the linear approximation (2.4), $C_i^{\text{eq}} \sim C_s(1 + \mu_i/T) \rightarrow C_s(1 + \mu/T) \sim C^{\text{eq}}$ where $C^{\text{eq}} = C_s e^{\mu/T}$ denotes the continuum-scale equilibrium density and μ is the respective chemical potential; cf. Corollary 4.4.

2.1.2. Desorption with zero drift. Now consider diffusion equation (2.1) with $v = 0$ and finite τ . The solution reads

$$(2.12) \quad C_i(x) = A_i e^{bx} + B_i e^{-bx}, \quad b := (D_s \tau)^{-1/2}.$$

The mass flux is $J_i(x) = -D_s \partial_x C_i = -D_s b(A_i e^{bx} - B_i e^{-bx})$. Boundary conditions (2.3) yield the matrix equation

$$(2.13) \quad \begin{pmatrix} e^{bx_i}(1 - \theta_u) & e^{-bx_i}(1 + \theta_u) \\ e^{bx_{i+1}}(1 + \theta_d) & e^{-bx_{i+1}}(1 - \theta_d) \end{pmatrix} \begin{pmatrix} A_i \\ B_i \end{pmatrix} = \begin{pmatrix} C_i^{\text{eq}} \\ C_{i+1}^{\text{eq}} \end{pmatrix},$$

where $\theta_\ell := D_s b/k_\ell$ ($\ell = u, d$). The mass flux on the i th terrace at $x = x_i$ is

$$(2.14) \quad J_i(x_i) = -D_s b \frac{C_{i+1}^{\text{eq}} - [\cosh(b \delta x_i) + \theta_d \sinh(b \delta x_i)] C_i^{\text{eq}}}{(1 + \theta_u \theta_d) \sinh(b \delta x_i) + (\theta_u + \theta_d) \cosh(b \delta x_i)}.$$

The flux at $x = x_{i+1}$ can be obtained by the interchanges $u \leftrightarrow d$ and $C_i^{\text{eq}} \leftrightarrow -C_{i+1}^{\text{eq}}$. The step velocities stem directly from (2.4)–(2.7).

In Appendix A, we outline the limit of (2.14) as $\delta x_i \downarrow 0$; see (A.2) and (A.3). We find that, if $D_s/(k_\ell a) = \mathcal{O}(1)$ and $a \ll k_\ell \tau$ ($\ell = u, d$), the effect of desorption is negligible since it is of higher order in the small scale a . This property is shown more generally in section 5.2 (see Remark 5.3). The resulting large-scale flux is given by the 1D version of (1.3) with $v = 0$, assuming that C^{eq} is linearized with μ via (2.4).

Remark 2.1. The fluxes in (2.11) and (2.14) are not simply proportional to $C_{i+1}^{\text{eq}} - C_i^{\text{eq}}$ (which in the macroscopic limit, $\delta x_i = x_{i+1} - x_i = \mathcal{O}(a) \downarrow 0$, becomes proportional to the gradient of the macroscale chemical potential μ). In section 4 we argue more generally that (2.11) and (2.14) reduce to different macroscopic laws for the flux: The electric-field drift has a distinct macroscopic signature in the resulting Fick's law; in contrast, the desorption effect is of higher order (in the expansion parameter a) and is deemed negligible for a broad class of materials and conditions.

2.1.3. Drift with desorption. Next, we solve the full equation (2.1). The density reads $C_i(x) = A_i e^{b_+ x} + B_i e^{-b_- x}$ where $b_\pm := \pm[b_v \pm \sqrt{b_v^2 + 4b^2}]/2 > 0$ and $b_v := v/D_s$. Boundary conditions (2.3) yield the system

$$(2.15) \quad \begin{pmatrix} e^{b_+ x_i}(1 - \theta_u^+ + v/k_u) & e^{-b_- x_i}(1 + \theta_u^- + v/k_u) \\ e^{b_+ x_{i+1}}(1 + \theta_d^+ - v/k_d) & e^{-b_- x_{i+1}}(1 - \theta_d^- - v/k_d) \end{pmatrix} \begin{pmatrix} A_i \\ B_i \end{pmatrix} = \begin{pmatrix} C_i^{\text{eq}} \\ C_{i+1}^{\text{eq}} \end{pmatrix},$$

where $\theta_i^\pm = D_s b_\pm / k_\ell$ ($\ell = u, d$). The i th-terrace mass flux at $x = x_i$ is

$$\begin{aligned}
 J_i(x_i) = & -\frac{D_s}{D_i^{\tau v}} \left\{ (b_+ + b_-) C_{i+1}^{\text{eq}} - \left([\theta_d^+ (b_v + b_-) e^{b+x} + \theta_d^- (b_v - b_+) e^{-b-x}] \right. \right. \\
 (2.16) \quad & \left. \left. + [(b_v + b_-) e^{b+x} - (b_v - b_+) e^{-b-x}] (1 - v/k_d) \right) C_i^{\text{eq}} \right\},
 \end{aligned}$$

where

$$\begin{aligned}
 D_i^{\tau v} = & (1 + \theta_d^+ - v/k_d) (1 + \theta_u^- + v/k_u) e^{b+\delta x_i} \\
 (2.17) \quad & - (1 - \theta_u^+ + v/k_u) (1 - \theta_d^- - v/k_d) e^{-b-\delta x_i}.
 \end{aligned}$$

In Appendix A, we sketch the macroscopic limit of (2.16). We find that desorption can plausibly be neglected compared to drift. More precisely, the sufficient conditions enabling this approximation include $v \ll k_\ell$ and $v/D_s \gg (k_\ell \tau)^{-1}$ ($\ell = u, d$), consistent with Remark 5.3, the analysis in [4], and the remarks in section 2.1.2. If the continuum-scale C^{eq} is linearized with μ , the resulting large-scale flux $J(x)$ is given by the 1D version of (1.3) for nonzero v ; cf. Corollary 4.4. More generally, by considering the nonlinear dependence of C^{eq} with μ , $C^{\text{eq}} = C_s e^{\mu/T}$ by (2.4), we obtain

$$(2.18) \quad J(x) = -D_s \frac{\partial_x C^{\text{eq}} - D_s^{-1} v C^{\text{eq}}}{1 + q|\partial_x h|} = -\frac{C_s D_s}{T} e^{\mu/T} \frac{\partial_x \mu - T D_s^{-1} v}{1 + q|\partial_x h|},$$

in agreement with the 1D form of (1.2) and the derivation of section 5.1.

The above microscopic model is consistent with the description invoked by Dufay, Frisch, and Debierre [4], who carry out a linear stability analysis under material deposition. Our focus here is the macroscopic limit of step flow, and thus our perspective differs from that in [4]. We recognize that, from a fully continuum view, deposition is special, leading to a different type of PDE, and is thus not touched upon here.

2.2. Concentric circular steps. In this section, we apply the BCF formulation to an axisymmetric setting. First, we aim to clarify details of the macroscopic limit by analogy with the methodology for zero drift followed in [28]. Second, since in actual experiments steps are curved, we view the radial geometry as a convenient (yet nontrivial) setting where drift and step curvature coexist and may compete.

So, consider steps that are concentric circles of radii $r_i(t)$ with $r_{i+1} > r_i$. The electric field \mathbf{E} is taken to be radial, viz., $\mathbf{E} = e_r E$ (e_r : radial unit vector) where E may vary with the polar coordinate r . To simplify the exposition, we set $E = \mathcal{E}(r)/r$.⁴

The electric field produces the radial drift velocity $\mathbf{v} = e_r v = e_r \mathcal{V}/r$ according to (1.1), where $\mathcal{V} = D_s Z^* e \mathcal{E}/T$. The radial adatom flux, $J_i(r) = e_r \cdot \mathbf{J}_i(r)$, is

$$(2.19) \quad J_i(r) = -D_s \partial_r C_i + v C_i \quad r_i < r < r_{i+1}.$$

The terrace diffusion equation under the quasi-steady approximation thus reads

$$(2.20) \quad 0 \approx -\text{div} \mathbf{J}_i - \tau^{-1} C_i = D_s (\partial_r^2 C_i + r^{-1} \partial_r C_i) - r^{-1} \mathcal{V} \partial_r C_i - r^{-1} (\partial_r \mathcal{V}) C_i - \tau^{-1} C_i$$

(where $r^{-1} (\partial_r \mathcal{V}) C_i = (\text{div} \mathbf{v}) C_i$). In the following, we neglect the term $r^{-1} (\partial_r \mathcal{V}) C_i$ assuming that, for $v \neq 0$, $|\partial_r \mathcal{V}| C_i \ll |\mathcal{V} \partial_r C_i|$; this holds, for example, if $\mathcal{V}(r)$ varies

⁴In experimental setups, \mathbf{E} must be generated and sustained by feasible charge distributions. The issue of sources for \mathbf{E} is not addressed here. These practical concerns suggest that the radial case here is a *toy model* for studying the interplay of drift and step curvature. We repeat that there is no physical principle forbidding rotational symmetry in future electromigration setups.

sufficiently slowly.⁵ Because of this approximation, (2.20) does not preserve terrace adatoms; i.e., adatoms in each terrace are not exactly balanced by fluxes at bounding steps. However, as pointed out in Remark 5.4 for 2D, in the macroscopic limit the effect of the neglected term is of higher order in a . Equation (2.20) becomes

$$(2.21) \quad 0 \approx D_s(\partial_r^2 C_i + r^{-1} \partial_r C_i) - r^{-1} \mathcal{V} \partial_r C_i - \tau^{-1} C_i.$$

Boundary conditions analogous to (2.3) that complement (2.21) follow from linear kinetics at the step edges:

$$(2.22) \quad -J_i(r_i) = k_u[C_i(r_i) - C_i^{\text{eq}}], \quad J_i(r_{i+1}) = k_d[C_i(r_{i+1}) - C_{i+1}^{\text{eq}}].$$

In this case, where steps have finite curvature, the equilibrium adatom density $C_i^{\text{eq}} \sim C_s(1 + \mu_i/T)$ contains information not only about the step interactions but also the energetic cost (line tension) of creating a step. The step chemical potential is [15, 28]

$$(2.23) \quad \mu_i = \frac{\Omega}{a} \left[\frac{\beta}{r_i} + \frac{1}{r_i} \partial_{r_i}(r_i U_i^{\text{int}}) \right],$$

where

$$(2.24) \quad U_i^{\text{int}} = g[V(r_i, r_{i+1}) + V(r_i, r_{i-1})],$$

$$(2.25) \quad V(r, r') = \frac{1}{3} \frac{2r'}{r+r'} \left(\frac{a}{r-r'} \right)^2,$$

β is the step line tension (assumed to be constant), and U_i^{int} is the interaction energy per unit length of the i th step; note the prefactor $\frac{2r'}{r+r'}$ for V in (2.25) [15].

The difference of fluxes from neighboring terraces at the i th step edge yields the step velocity $\dot{r}_i = \frac{dr_i}{dt}$ according to mass conservation,

$$(2.26) \quad \dot{r}_i = \frac{\Omega}{a} [J_{i-1}(r_i) - J_i(r_i)].$$

The coupled step flow equations with drift and desorption form an extension of the axisymmetric model by Israeli and Kandel [15] and Fok [10].

Next, we study the case with $\tau \rightarrow \infty$, where explicit radial solutions are relatively simple. This case suffices for our purposes. A more general discussion including desorption in full 2D can be found in section 5.2.

2.2.1. Electric-field solution with no desorption. We solve (2.21) for $\tau \rightarrow \infty$. By successive integrations we obtain the formula

$$(2.27) \quad C_i(r) = B_i + A_i \int_{r_i}^r \frac{1}{z} \exp \left[D_s^{-1} \int_{r_i}^z v(r') dr' \right] dz \quad r_i < r < r_{i+1}.$$

By (2.19), we compute the corresponding (radial) flux:

$$(2.28) \quad J_i(r) = A_i \left\{ -\frac{D_s}{r} \exp \left[D_s^{-1} \int_{r_i}^r v(r') dr' \right] + v(r) \int_{r_i}^r \frac{1}{z} \exp \left[D_s^{-1} \int_{r_i}^z v(r') dr' \right] dz \right\} + v(r) B_i.$$

⁵This condition is also expected to hold for \mathcal{V} of the form $\mathcal{V} = cr^\omega$ with sufficiently large r .

Substituting (2.27) and (2.28) for C_i and J_i in conditions (2.22), we find

$$(2.29) \quad \begin{pmatrix} -\frac{D_s}{k_u r_i} & 1 + \frac{v_i}{k_u} \\ \left(1 - \frac{v_{i+1}}{k_d}\right) \int_{r_i}^{r_{i+1}} \phi_i(z) dz + \frac{D_s}{k_d} \phi_i(r_{i+1}) & 1 - \frac{v_{i+1}}{k_d} \end{pmatrix} \begin{pmatrix} A_i \\ B_i \end{pmatrix} = \begin{pmatrix} C_i^{\text{eq}} \\ C_{i+1}^{\text{eq}} \end{pmatrix},$$

where $v_j := v(r_j)$ ⁶ and

$$(2.30) \quad \phi_i(r) := \frac{1}{r} \exp \left[D_s^{-1} \int_{r_i}^r v(r') dr' \right].$$

Solving for A_i and B_i we have

$$(2.31) \quad A_i = \frac{\mathcal{D}_A}{\mathcal{D}^v}, \quad B_i = \frac{\mathcal{D}_B}{\mathcal{D}^v},$$

$$(2.32) \quad \mathcal{D}^v := \frac{D_s}{k_u r_i} \left(1 - \frac{v_{i+1}}{k_d}\right) + \left[\frac{D_s}{k_d} \phi_i(r_{i+1}) + \left(1 - \frac{v_{i+1}}{k_d}\right) \int_{r_i}^{r_{i+1}} \phi_i(z) dz \right] \times \left(1 + \frac{v_i}{k_u}\right),$$

$$(2.33) \quad \mathcal{D}_A := \left(1 + \frac{v_i}{k_u}\right) C_{i+1}^{\text{eq}} - \left(1 - \frac{v_{i+1}}{k_d}\right) C_i^{\text{eq}},$$

$$(2.34) \quad \mathcal{D}_B := \frac{D_s}{k_u r_i} C_{i+1}^{\text{eq}} + \left[\frac{D_s}{k_d} \phi_i(r_{i+1}) + \left(1 - \frac{v_{i+1}}{k_d}\right) \int_{r_i}^{r_{i+1}} \phi_i(z) dz \right] C_i^{\text{eq}}.$$

The above formulas are simplified considerably if rv is treated as a constant.

For $r = r_i$ the radial flux reads

$$(2.35) \quad J_i(r_i) = -\frac{D_s A_i}{r_i} + v_i B_i.$$

The value $J_{i-1}(r_i)$ can be obtained similarly. The step velocities are described by (2.23)–(2.26), given that $C_i^{\text{eq}} \sim C_s(1 + \mu_i/T)$.

In Appendix A we outline the full continuum limit of (2.35), as $r_{i+1} - r_i = \mathcal{O}(a) \downarrow 0$; see (A.5). The resulting, large-scale flux is found in agreement with the radial version of (1.3) when C^{eq} is linearized with μ via (2.4); see also Corollary 4.4.

We conclude this subsection by noting in passing that the term $(\text{div} \mathbf{v})C_i$, which was neglected above, can be included in the diffusion equation without difficulty (although the algebra is lengthier and less transparent). An idea is to treat the term in question as a forcing, apply Duhamel’s principle and thus derive an integral equation for C_i , which can be solved via a Born–Neumann series by iteration. This approach is undertaken in section 5.2 for 2D; see Remark 5.4. Alternatively, C_i can be expressed in terms of confluent hypergeometric functions [7].

3. 2D step model. In this section, we consider steps of reasonably arbitrary shape and formulate their equations of motion under a macroscopic electric field \mathbf{E} without desorption ($\tau = \infty$, i.e., $b = (D_s \tau)^{-1/2} = 0$). Of particular interest are unidirectional electric fields with magnitudes that vary over a length scale large compared to the typical width of a terrace. So, we impose

$$(3.1) \quad |(\text{div} \mathbf{v}) C_i| \ll |\mathbf{v} \cdot \nabla C_i|.$$

⁶This distinction is redundant if $v(r)$ is macroscopic; i.e., it varies slowly.

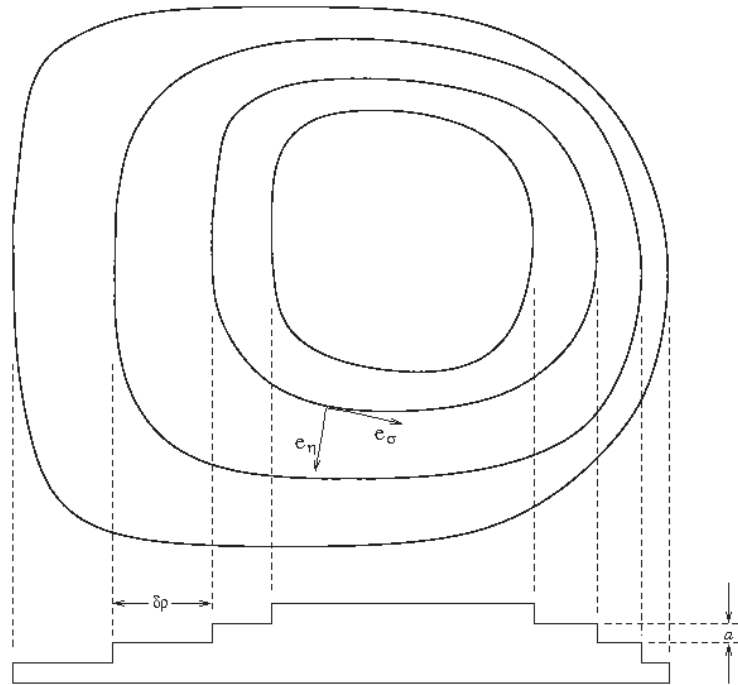


FIG. 3.1. Schematic (top and side views) of steps; a is the (microscopic) step height, $e_\eta \cdot e_\sigma = 0$, and $\delta\rho = \delta\rho_i := \int_{\eta_i}^{\eta_{i+1}} \xi_\eta \, d\eta$ is the terrace width. On top, steps are projected on a reference plane.

Condition (3.1) is satisfied trivially by $\operatorname{div} \mathbf{v} \equiv 0$, e.g., if \mathbf{E} is constant, which corresponds to many experimentally relevant situations.⁷ The neglect of the $(\operatorname{div} \mathbf{v})C_i$ term in the diffusion equation leads to, strictly speaking, violation of mass conservation at the level of terrace adatoms (i.e., adatoms lost or gained in each terrace are not exactly balanced by fluxes at the bounding step edges). However, as pointed out in Remark 5.4, at the macroscale the corresponding correction for the adatom flux is negligibly small (being of higher order in a).

With regard to the actual step geometry, we assume that the step edges are represented by smooth, closed curves on the reference plane (x, y) , which do not cross or self-intersect, as is ensured physically by the step-step repulsive (entropic and elastic dipole) interactions.

3.1. Step geometry. We now describe the step configuration in more detail. The step train is monotonic, with steps descending outward from a top terrace (surface peak); see Figure 3.1. Their edges are numbered $1, 2, \dots, N$, starting from the topmost step. Following [25, 28], we introduce local coordinates (η, σ) : The nondimensional coordinate η identifies the step edges and measures their distance from a reference point on the top terrace; the i th step edge is the level set $\eta = \eta_i$, and the i th terrace is the region $\eta_i < \eta < \eta_{i+1}$. The coordinate σ measures the location along a step edge; for definiteness, we take σ to increase counterclockwise (top view). The unit vectors e_η and e_σ are orthogonal, in the direction of increasing η and σ , respectively. The

⁷If the three-dimensional \mathbf{E} inducing surface electromigration depends only on (x, y) , the coordinates in the reference (high-symmetry) plane, then (3.1) is trivially satisfied (by $\operatorname{div} \mathbf{v} \equiv 0$) in the absence of charge distribution. In this case, $\operatorname{curl} \mathbf{v} = 0$ for a static field.

relevant metric coefficients are defined by

$$\xi_\eta := |\partial_\eta \mathbf{r}|, \quad \xi_\sigma := |\partial_\sigma \mathbf{r}| \quad [\mathbf{r} = (x, y) : \text{position vector}].$$

In the following, ξ_η and ξ_σ are treated as $\mathcal{O}(1)$ and slowly varying with σ .

3.2. Equations of motion. In view of (3.1) and the quasi-steady approximation, the adatom density field C_i in the i th-terrace region ($\eta_i < \eta < \eta_{i+1}$) solves

$$(3.2) \quad 0 \approx \partial_t C_i = \text{div}(\mathbf{D}_s \cdot \nabla C_i) - \mathbf{v} \cdot \nabla C_i, \quad \nabla = (\partial_x, \partial_y) = (\xi_\eta^{-1} \partial_\eta, \xi_\sigma^{-1} \partial_\sigma),$$

where \mathbf{D}_s is in principle a tensor function of position \mathbf{r} . Here, we consider a scalar constant, $\mathbf{D}_s = D_s$; see section 5.3 for anisotropic terrace diffusion. The (vector-valued) adatom flux \mathbf{J}_i is

$$(3.3) \quad \mathbf{J}_i = -D_s \nabla C_i + \mathbf{v} C_i.$$

Robin-type boundary conditions for (3.2) inform C_i of the following: (i) attachment and detachment of atoms at steps; and (ii) step energetics, especially step-step interactions, via the equilibrium concentration, C_i^{eq} . These boundary conditions read

$$(3.4) \quad -J_{i,\perp}(\eta_i, \sigma) = k_u [C_i(\eta_i, \sigma) - C_i^{\text{eq}}(\sigma)],$$

$$(3.5) \quad J_{i,\perp}(\eta_{i+1}, \sigma') = k_d [C_i(\eta_{i+1}, \sigma') - C_{i+1}^{\text{eq}}(\sigma')]; \quad J_{i,\perp} := e_\eta \cdot \mathbf{J}_i, \quad k_u/k_d = \mathcal{O}(1).$$

Recall that each step advances or retreats according to the locally incoming and outgoing normal fluxes. This mass conservation is expressed by the step velocity law

$$(3.6) \quad v_i = e_\eta \cdot \frac{d\mathbf{r}_i}{dt} = \frac{\Omega}{a} (J_{i-1,\perp} - J_{i,\perp}) \quad \eta = \eta_i.$$

To determine $J_{i,\perp}$, we need to address the energetics of a step train, i.e., express C_i^{eq} by (2.4) in terms of step positions. This is discussed for 2 + 1 dimensions in [28]. We briefly review these energetic considerations. The step free energy $E^N = E^N(\{\mathbf{r}_i\})$ (N : number of steps) is defined by

$$(3.7) \quad E^N = \sum_{i=1}^N \int_{L_i} ds (\beta + gV_{i,i+1}),$$

where L_i is the i th-step curve, β is the step line tension, and $gV_{i,i+1}$ expresses the elastic dipole and entropic step-step interaction. Following [28], we further introduce $V_{i,i+1} = (1/3) m_i^2 \Phi(\zeta_i, \zeta_{i+1})$, where Φ is a shape factor, m_i is the step density, and $\zeta_i = \rho_i/\lambda$ is the nondimensional step position (λ : macroscopic length); $\rho = \int_0^\eta \xi_{\eta'} d\eta'$ is the distance from the origin measured along a σ -level curve.

The step chemical potential, μ_i , is defined by

$$(3.8) \quad \mu_i = \Omega \frac{\delta E^N}{\delta \rho_i},$$

the variation of E^N . The equilibrium concentration C_i^{eq} is determined by (2.4).

3.3. Approximate solution of diffusion equation. By use of the local coordinates (η, σ) , diffusion equation (3.2) for $C_i(\eta, \sigma)$ reads

$$(3.9) \quad 0 = \frac{D_s}{\xi_\eta \xi_\sigma} \left[\partial_\eta \left(\frac{\xi_\sigma}{\xi_\eta} \partial_\eta C_i \right) + \partial_\sigma \left(\frac{\xi_\eta}{\xi_\sigma} \partial_\sigma C_i \right) \right] - v_\perp \xi_\eta^{-1} \partial_\eta C_i - v_\parallel \xi_\sigma^{-1} \partial_\sigma C_i,$$

where $\eta_i < \eta < \eta_{i+1}$; $v_\perp := e_\eta \cdot \mathbf{v}$ and $v_\parallel := e_\sigma \cdot \mathbf{v}$.

By analogy with the case of zero electric field [28], we solve (3.9) with recourse to the following proposition (which forms an extension of the procedure applied in [28]).

PROPOSITION 3.1. Consider the boundary value problem consisting of PDE (3.9) on the terrace $U_i = \{(\eta, \sigma) \mid \eta_i < \eta < \eta_{i+1}\}$, and conditions (3.4) and (3.5) on the boundary, ∂U_i , of U_i . Suppose the following: (i) the boundary data exhibit a scale separation in the sense that, for some geometric parameter $\epsilon \ll 1$, C_i^{eq} is a fixed, $\mathcal{O}(1)$ function of the slow variable $\tilde{\sigma} := \epsilon\sigma$, i.e., $C_i^{\text{eq}} = C_i^{\text{eq}}(\tilde{\sigma})$, while the rates k_u, k_d are ϵ -independent; (ii) the metric coefficients ξ_η and ξ_σ depend on $(\eta, \tilde{\sigma})$ and are $\mathcal{O}(1)$ as $\epsilon \downarrow 0$; and (iii) $\text{curl } \mathbf{v} = 0$ (i.e., $\partial_x v_y = \partial_y v_x$)⁸ and $\min\{k_u, k_d\} > (1/2)|\mathbf{v}|$. Let C_i be a C^2 (twice continuously differentiable) function on U_i and C^1 (continuously differentiable) function on \bar{U}_i , the closure of U_i . Then, for $\eta = \mathcal{O}(1)$, $C_i(\eta, \sigma) = C_i^{(0)}(\eta, \tilde{\sigma}) + o(1)$ where

$$(3.10) \quad C_i^{(0)}(\eta, \tilde{\sigma}) = B_i(\tilde{\sigma}) + A_i(\tilde{\sigma}) \int_{\eta_i}^\eta dz \frac{\xi_\eta|z}{\xi_\sigma|z} \exp \left[\int_{\eta_i}^z \frac{(v_\perp \xi_\eta)|\eta'}{D_s} d\eta' \right],$$

and $o(1) \rightarrow 0$ as $\epsilon \downarrow 0$. The integration constants A_i and B_i are given by

$$(3.11) \quad A_i(\tilde{\sigma}) = \frac{(1 + v_\perp|_{\eta_i}/k_u)C_{i+1}^{\text{eq}} - (1 - v_\perp|_{\eta_{i+1}}/k_d)C_i^{\text{eq}}}{\frac{D_s}{k_u \xi_\sigma|_{\eta_i}} \left(1 - \frac{v_\perp|_{\eta_{i+1}}}{k_d} \right) + \left(1 + \frac{v_\perp|_{\eta_i}}{k_u} \right) \left[\frac{D_s}{k_d \xi_\eta} \partial_\eta f_i|_{\eta_{i+1}} + \left(1 - \frac{v_\perp}{k_d} \right) f_i|_{\eta_{i+1}} \right]},$$

$$(3.12) \quad B_i(\tilde{\sigma}) = \left(1 + \frac{v_\perp|_{\eta_i}}{k_u} \right)^{-1} \left[C_i^{\text{eq}}(\tilde{\sigma}) + \frac{D_s}{k_u \xi_\sigma|_{\eta_i}} A_i(\tilde{\sigma}) \right],$$

where $f_i(\eta, \sigma)$ is defined by

$$(3.13) \quad f_i(\eta, \sigma) := \int_{\eta_i}^\eta \frac{\xi_\eta|z}{\xi_\sigma|z} \exp \left[\int_{\eta_i}^z \frac{(v_\perp \xi_\eta)|\eta'}{D_s} d\eta' \right] dz \quad (\eta, \sigma) \in U_i.$$

In the above, $Q|_z$ denotes the value $Q(\eta = z)$. The role of parameter ϵ is to express small variations of the step edge curvature, which in turn cause slow variations of $C_i = C_i^\epsilon(\eta, \sigma)$ with respect to σ , permitting a perturbative treatment. In the limit $\epsilon \downarrow 0$, the step edges become 1D, approaching concentric circles or straight lines (depending on limits of ξ_η and ξ_σ). We also assume that k_u and k_d are positive (as is typical in crystalline materials). For comments on the condition $|\mathbf{v}|/k_\ell < 2$ where $\ell = u, d$, see Remark 3.2; note that in many physical situations $|\mathbf{v}| \ll k_\ell$ [4].

Proof. For convenience and notational economy, in this proof we set $D_s = 1$ (or, define the inverse length $\hat{\mathbf{v}} := \mathbf{v}/D_s$ and drop the hat) and suppress the terrace index i unless noted otherwise. Assuming that a solution $C(\mathbf{r}) = C^\epsilon(\mathbf{r})$ exists and is unique, as implied below, we partly separate scales in PDE (3.9) for $\eta = \mathcal{O}(1)$. So, we expand formally $C^\epsilon(\mathbf{r})$ in an ϵ -power series; each coefficient, $C^{(j)}$, is allowed to be a function

⁸Alternatively, it can be assumed that $\mathbf{v}(\mathbf{r})$ varies slowly, e.g., $\mathbf{v} = \mathbf{v}(\epsilon_1 \eta, \epsilon_1 \sigma)$, $\epsilon_1 \ll \epsilon$.

of $(\eta, \sigma, \tilde{\sigma})$ which are treated as independent variables:⁹

$$(3.14) \quad C^\epsilon(\eta, \sigma) = C^{(0)}(\eta, \sigma, \tilde{\sigma}) + \sum_{j \geq 1} \epsilon^j C^{(j)}(\eta, \sigma, \tilde{\sigma}) = C^{(0)}(\eta, \sigma, \tilde{\sigma}) + o(1),$$

where the remainder approaches 0 as $\epsilon \downarrow 0$, using continuity of the solution with ϵ .¹⁰ In addition, the operator ∂_σ is replaced by the linear combination

$$\partial_\sigma \Rightarrow \partial_\sigma + \epsilon \partial_{\tilde{\sigma}}.$$

By dominant balance of $\mathcal{O}(\epsilon^0)$ terms, (3.9) entails the (zeroth-order) PDE

$$(3.15) \quad \left\{ \frac{1}{\xi_\eta \xi_\sigma} \left[\partial_\eta \left(\frac{\xi_\sigma}{\xi_\eta} \partial_\eta \right) + \partial_\sigma \left(\frac{\xi_\eta}{\xi_\sigma} \partial_\sigma \right) \right] - v_\perp \frac{\partial_\eta}{\xi_\eta} - v_\parallel \frac{\partial_\sigma}{\xi_\sigma} \right\} C^{(0)} = 0 \quad (\mathbf{r} \in U),$$

which must be solved under conditions (3.4) and (3.5) for $C^{(0)}$ (for ϵ -independent k_u and k_d).

Next, we show that, for given continuous $C^{\text{eq}}(\tilde{\sigma})$, the above boundary value problem for $C^{(0)}$ has at most one solution. We apply a standard energy method [9]; the same argument carries through for proving uniqueness of C^ϵ . First, by the transformation $C^{(0)} = \check{C} e^{(1/2) \int_{\mathbf{r}_i}^{\mathbf{r}} \mathbf{v} \cdot d\mathbf{r}'}$, PDE (3.15) is converted to the Helmholtz equation $\Delta_{\mathbf{r}} \check{C} - \frac{1}{4}(|\mathbf{v}|^2 - 2\text{div}\mathbf{v})\check{C} = 0$ ($\mathbf{r} \in U$: terrace), where \check{C} obeys the Robin boundary condition $-\nu \cdot \nabla \check{C} =: -\partial_\nu \check{C} = K(\mathbf{r})\check{C} - k(\mathbf{r})C^{\text{eq}} e^{-(1/2) \int_{\mathbf{r}_i}^{\mathbf{r}} \mathbf{v} \cdot d\mathbf{r}'}$ ($\mathbf{r} \in \partial U$); ν is the unit outward normal vector, $K(\mathbf{r}) := k(\mathbf{r}) - (1/2)\nu \cdot \mathbf{v}$, and $k(\mathbf{r}) = k_u$ for an up-step edge ($\eta = \eta_i$ where $\nu = -e_\eta$) while $k(\mathbf{r}) = k_d$ for a down-step edge ($\eta = \eta_{i+1}$ where $\nu = e_\eta$). Consider sufficiently small $|\mathbf{v}|$ so that $K(\mathbf{r}) > 0$, yet $|\mathbf{v}|^2 \geq 2\text{div}\mathbf{v}$, consistent with the neglect of the term $(\text{div}\mathbf{v})C^\epsilon$ in the diffusion equation. Now suppose there exist two solutions, say \check{C}_1 and \check{C}_2 , of the boundary problem for $C^{(0)}$, with $\varphi := \check{C}_1 - \check{C}_2$; this φ satisfies the given Helmholtz equation with boundary condition $-\partial_\nu \varphi = K \varphi$. Second, define the nonnegative energy $\mathcal{E}[\varphi] = \frac{1}{2} \int_U |\nabla \varphi|^2 + \varpi^2 \varphi^2$ where $\varpi^2 := (1/4)(|\mathbf{v}|^2 - 2\text{div}\mathbf{v})$. By Green's identity, $\mathcal{E}[\varphi] = \int_{\partial U} (\nu \cdot \nabla \varphi) \varphi = - \int_{\partial U} K \varphi^2 \leq 0$; thus, $\varphi \equiv 0$ which entails $C_1 \equiv C_2$.

Based on this uniqueness assertion, we construct solution (3.10)–(3.12). The $\tilde{\sigma}$ -dependence of C^{eq} in the boundary data suggests that we look for a $C^{(0)}(\mathbf{r})$ that depends on η and $\tilde{\sigma}$ (but not σ). Such a $C^{(0)}(\mathbf{r})$, if it can be constructed plausibly, is interpreted as the leading-order, unique solution of the boundary value problem.

Hence, we solve (3.15) by dropping the σ -derivatives. Two successive integrations with respect to the variable η immediately yield

$$(3.16) \quad C^{(0)}(\eta, \tilde{\sigma}) = B(\tilde{\sigma}) + \hat{A}(\tilde{\sigma}) \int_{\eta_i}^\eta \exp \left\{ - \int_{\eta_i}^z \left[\frac{\xi_{\eta'}}{\xi_\sigma} \partial_{\eta'} \left(\frac{\xi_\sigma}{\xi_{\eta'}} \right) - \frac{(v_\perp |\eta'|) \xi_{\eta'}}{D_s} \right] d\eta' \right\} dz,$$

where \hat{A} and B are integration constants. Equation (3.16) readily reduces to (3.10) by direct integration (in η') of the first term in the exponent and the subsequent substitution $A(\tilde{\sigma}) := (\xi_\sigma / \xi_\eta)|_{\eta_i} \hat{A}(\tilde{\sigma})$.

The coefficients $A(\tilde{\sigma})$ and $B(\tilde{\sigma})$ are determined through boundary conditions (3.4) and (3.5) with $\sigma = \sigma'$. Accordingly, we obtain the system

$$\begin{pmatrix} -\frac{D_s}{k_u \xi_\sigma |_{\eta_i}} & 1 + \frac{v_\perp |\eta_i|}{k_u} \\ \frac{D_s}{k_d \xi_\eta} \partial_\eta f|_{\eta_{i+1}} + (1 - v_\perp / k_d) f|_{\eta_{i+1}} & 1 - \frac{v_\perp |\eta_{i+1}|}{k_d} \end{pmatrix} \begin{pmatrix} A \\ B \end{pmatrix} = \begin{pmatrix} C_i^{\text{eq}} \\ C_{i+1}^{\text{eq}} \end{pmatrix},$$

⁹The use of the extra slow variable $\tilde{\eta} = \epsilon \eta$, although formally justifiable, is not deemed necessary.

¹⁰This physical property is invoked in conjunction with the assumption that eliminating the curvature variation (as $\epsilon \downarrow 0$) results in a well-defined adatom density, as suggested by section 2.

where $f(\eta, \sigma)$ is defined by (3.13). Solving this system leads to (3.11) and (3.12). \square

Henceforth, we drop the dependence of $v_\perp = \mathbf{v} \cdot e_\eta$ (and $v_\parallel = e_\sigma \cdot \mathbf{v}$) on i , since \mathbf{v} is considered macroscopic and e_η and e_σ vary slowly with η . It can be verified that (3.10) reduces to the solutions for 1D settings of sections 2.1.1 and 2.2.1.

Remark 3.2. Thus far, we invoked the condition $|\mathbf{v}|/k_\ell < 2$ ($\ell = u, d$). By definition (1.1) for \mathbf{v} , this restriction amounts to imposing

$$\frac{|\mathbf{v}|}{2k_\ell} = \frac{D_s}{2k_\ell a} \frac{|Z^* \epsilon| |\mathbf{E}| a}{T} < 1, \quad \ell = u, d.$$

In typical experimental situations, $D_s/(2k_\ell a)$ is of the order of 10^2 or smaller [16], $|\mathbf{E}|a/T$ is of the order of 10^{-5} , and $|Z^*|$ ranges from 10^{-4} (or even smaller values) to about 10 [4, 13]. Hence, $|\mathbf{v}|/k_\ell$ would not exceed values of the order of 10^{-2} . From the perspective of perturbation theory adopted here, $D_s/(k_\ell a)$ is treated as an $\mathcal{O}(1)$ quantity, whereas $|\mathbf{v}|/k_\ell$ will be considered as $o(1)$ (see Proposition 4.1) when $a \downarrow 0$. Physically, this means that the drift of adatoms is slow compared to the atom attachment-detachment at steps. This assumption is consistent with the numerical values implemented in recent studies, e.g., [4]. Practically, setting $|\mathbf{v}| \ll k_\ell$ appears to more closely describe semiconductor surfaces, where $|Z^*|$ can be much smaller than unity [13]. Mathematically, this view offers a convenient choice for obtaining the distinguished-limit contribution of \mathbf{v} as $a \downarrow 0$.

In section 4.2 we impose $|\mathbf{v}|/k_\ell \ll 1$; as a result, Fick's law for the large-scale flux does not distinguish between up- and down-step edges, being symmetric in k_u and k_d .

4. Macroscopic limit in 2D. In this section, we derive the macroscopic limit of step motion laws by regarding step flow as a discrete scheme for a PDE satisfied by the surface height h . Our main task is to extract this PDE. Three essential relations contribute to macroscale relaxation: (i) the mass conservation law, which emerges from the limit of step velocity (3.6); (ii) the step chemical potential in terms of the surface height gradient, which follows from the energy of a step train, (3.7); and (iii) the constitutive relation (Fick's law) between adatom flux and step chemical potential, which follows from (3.3)–(3.5), by account of the drift (linear-in- \mathbf{v}) term.

Relations (i), (ii), and (iii) *without an electric field* ($\mathbf{v} = 0$) have been well established [28]; in particular, (i) and (ii) were derived from a strong and a weak formulation standpoint. In contrast, macroscopic relation (iii) in the presence of an electric field has apparently not been addressed adequately.

4.1. Mass conservation and step chemical potential. Next, we review briefly relations (i) and (ii) mentioned above, which do *not* depend upon the electric field. The law of mass conservation, in the absence of edge atom diffusion [39] and material deposition from above, reads

$$(4.1) \quad \partial_t h + \Omega \operatorname{div} \mathbf{J} = 0,$$

where Ω is the atomic volume and $\mathbf{J}(\mathbf{r}, t)$ is the macroscale surface flux. Equation (4.1) stems directly from (3.6) via the limit $e_\eta \cdot \mathbf{r}_i \rightarrow \partial_t h / |\nabla h|$ as $a \downarrow 0$ (since each terrace is a level set for h); for details, see [28].

The macroscale chemical potential μ is regarded as a smooth interpolation, through a suitable Taylor expansion, of the microscale step chemical potential μ_i . In the weak sense, μ can be expressed as the first variation in L^2 of the macroscale surface free energy $E = \lim_{N \rightarrow \infty} E^N$, which comes from (3.7) via the limit $a \sum_i \rightarrow \int dh$ and the

coarea formula [28]. This E takes the form (1.4) with $g_1 = \beta/a$ and $g_3 = (g/a)\Phi_0$ where $\Phi_o = \Phi(\zeta_i, \zeta_i)$. Hence, the chemical potential reads [28]¹¹

$$(4.2) \quad \mu = \Omega \left(\frac{\delta E}{\delta h} \right)_{L^2} = -\Omega \operatorname{div} \left\{ \partial_m [m(g_1 + g_3 m^2)] \frac{\nabla h}{|\nabla h|} \right\}, \quad m := |\nabla h|.$$

4.2. Macroscopic Fick’s law with drift. In this section, we derive the constitutive relation between macroscale flux and chemical potential in full 2D. The restrictions to 1D geometries then follow as special cases. We choose units where the macroscopic length λ is unity ($\lambda = 1$) for convenience.

PROPOSITION 4.1. *Suppose that in the macroscopic limit, $a \downarrow 0$, the step density $m_i = a/(\xi_\eta \delta \eta_i)$ and the kinetic parameters $D_s/(k_\ell a)$ are $\mathcal{O}(1)$ while $v/k_\ell = o(1)$, where $\ell = u, d$ and $\delta \eta_i := \eta_{i+1} - \eta_i$. Then, the solution to (3.9) under boundary conditions (3.4) and (3.5) gives rise to the macroscale constitutive relation*

$$(4.3) \quad \mathbf{J} = \begin{pmatrix} J_\perp \\ J_\parallel \end{pmatrix} = -C_s \mathbf{M} \cdot \left[\nabla \mu - \frac{T}{D_s} \mathbf{v} \left(1 + \frac{\mu}{T} \right) \right] \quad \left(\mathbf{v} = \frac{D_s Z^* e \mathbf{E}}{T} \right),$$

where the (\mathbf{E} -independent) mobility \mathbf{M} (with units of $\text{length}^2/\text{energy}/\text{time}$) is a second-rank tensor. In the coordinate system (η, σ) , this \mathbf{M} has the representation [28]

$$(4.4) \quad \mathbf{M} = \frac{D_s}{T} \frac{1}{1 + q|\nabla h|} \begin{pmatrix} 1 & 0 \\ 0 & 1 + q|\nabla h| \end{pmatrix}, \quad q := \frac{2D_s}{ka}, \quad k := \frac{2}{k_u^{-1} + k_d^{-1}}.$$

Proof. The starting point is the solution $C_i^{(0)}$ derived in Proposition 3.1; see (3.10). We drop the superscript (denoting perturbation order) in $C_i^{(0)}$ for ease of notation. The microscale adatom flux components are obtained by the formulas

$$\begin{aligned} J_{i,\parallel} &= -D_s \xi_\sigma^{-1} \partial_\sigma C_i + v_\parallel C_i, \\ J_{i,\perp} &= -D_s \xi_\eta^{-1} \partial_\eta C_i + v_\perp C_i. \end{aligned}$$

The plan is to consider the restrictions of these components to $\eta = \eta_i$, and view these restrictions as interpolations of (continuous) smooth functions, $J_\perp(\mathbf{r}, t)$ and $J_\parallel(\mathbf{r}, t)$.

First, we compute the requisite derivatives of C_i by (3.10):

$$\begin{aligned} \partial_\sigma C_i &\sim \partial_\sigma B_i + \partial_\sigma A_i \int_{\eta_i}^\eta \frac{\xi_\eta|z}{\xi_\sigma|z} \exp \left[\int_{\eta_i}^z \frac{\xi_{\eta'} v_\perp | \eta'}{D_s} d\eta' \right] dz, \\ \partial_\eta C_i &= A_i \frac{\xi_\eta}{\xi_\sigma} \exp \left[\int_{\eta_i}^\eta \frac{\xi_{\eta'} (v_\perp | \eta')}{D_s} d\eta' \right]. \end{aligned}$$

It follows that

$$(4.5) \quad J_{i,\parallel} = -D_s \xi_\sigma^{-1} \partial_\sigma B_i + v_\parallel B_i,$$

$$(4.6) \quad J_{i,\perp} = -D_s \xi_\sigma^{-1} A_i + v_\perp B_i \quad \eta = \eta_i.$$

Consider (3.11) and (3.12) (of Proposition 3.1) for A_i and B_i . In the limit $a \downarrow 0$, or $\delta \eta_i \downarrow 0$ with $\xi_\eta \delta \eta_i = \mathcal{O}(a)$, these formulas simplify via the expansion $\int_{\eta_i}^{\eta_i + 1} F(\eta) d\eta =$

¹¹In carrying out the variational derivative of E , it is commonly assumed that boundary terms vanish, e.g., by fixing the height h at the boundary or applying periodic boundary conditions.

$F(\eta_i) \delta\eta_i + o(\delta\eta_i)$, where $F(\eta)$ is any continuous function. After some algebra and neglect of $o(\delta\eta_i)$ terms, (4.5) and (4.6) become

$$(4.7) \quad J_{i,\parallel}|_{\eta_i} \sim \frac{v_{\parallel} \left[\frac{D_s}{\xi_{\eta} \delta\eta_i} \left(\frac{C_i^{\text{eq}}}{k_d} + \frac{C_{i+1}^{\text{eq}}}{k_u} \right) + C_i^{\text{eq}} \right] - D_s \left[\partial_{\parallel} C_i^{\text{eq}} + \frac{D_s}{\xi_{\eta} \delta\eta_i} \left(\frac{\partial_{\parallel} C_i^{\text{eq}}}{k_d} + \frac{\partial_{\parallel} C_{i+1}^{\text{eq}}}{k_u} \right) \right]}{\frac{D_s}{\xi_{\eta} \delta\eta_i} \left(\frac{1}{k_u} + \frac{1}{k_d} \right) + \left(1 + \frac{v_{\perp}}{k_u} \right)},$$

$$(4.8) \quad J_{i,\perp}|_{\eta_i} \sim \frac{\frac{D_s}{\xi_{\eta} \delta\eta_i} (C_i^{\text{eq}} - C_{i+1}^{\text{eq}}) + v_{\perp} C_i^{\text{eq}}}{\frac{D_s}{\xi_{\eta} \delta\eta_i} \left(\frac{1}{k_u} + \frac{1}{k_d} \right) + \left(1 + \frac{v_{\perp}}{k_u} \right)} \quad \text{as } \delta\eta_i \downarrow 0; \quad \partial_{\parallel} := \xi_{\sigma}^{-1} \partial_{\sigma}.$$

In the above, all variables are evaluated at (the same) σ along the i th step edge.

We seek further simplification of (4.7) and (4.8). In the macroscopic limit, we invoke the (assumed as well defined) C^1 function $C^{\text{eq}}(\mathbf{r})$ where $C^{\text{eq}}(\mathbf{r})|_{\eta_i} \equiv C_i^{\text{eq}}$, $C_{i+1}^{\text{eq}} \equiv C^{\text{eq}}(\mathbf{r})|_{\eta_i} + (\partial_{\eta} C^{\text{eq}})|_{\eta_i} \delta\eta_i + o(\delta\eta_i)$, and $\partial_{\parallel} C^{\text{eq}}|_{\eta_i} \equiv \partial_{\parallel} C_i^{\text{eq}} = \partial_{\parallel} C_{i+1}^{\text{eq}} + O(\delta\eta_i)$. We keep only those combinations of microscopic parameters that remain $O(1)$. For example, the step density $m_i = a/(\xi_{\eta} \delta\eta_i)$ approaches the positive surface slope, i.e., $\lim_{a \downarrow 0} m_i = |\nabla h|$. On the other hand, the ratio v_{\perp}/k_u , involved in the denominator of $J_{i,\parallel}$ and $J_{i,\perp}$, is treated as negligibly small (compared to unity) by virtue of our hypothesis; see also Remark 3.2.

Without further ado, we make the substitutions $C_{i+1}^{\text{eq}} - C_i^{\text{eq}} = (\partial_{\perp} C^{\text{eq}}) \xi_{\eta} \delta\eta_i + o(\delta\eta_i)$ and $C^{\text{eq}} \sim C_s(1 + \mu/T)$ ($|\mu| \ll T$), where $\partial_{\perp} := \xi_{\eta}^{-1} \partial_{\eta}$. The resulting limits for the flux components read

$$(4.9) \quad \lim_{a \downarrow 0} J_{i,\parallel}|_{\eta_i} =: J_{\parallel}(\mathbf{r})|_{\eta_i} = -\frac{C_s D_s}{T} \partial_{\parallel} \mu(\mathbf{r}) + C_s v_{\parallel} \left[1 + \frac{\mu(\mathbf{r})}{T} \right],$$

$$(4.10) \quad \lim_{a \downarrow 0} J_{i,\perp}|_{\eta_i} =: J_{\perp}(\mathbf{r})|_{\eta_i} = -\frac{C_s D_s}{T} \frac{\partial_{\perp} \mu - \frac{T}{D_s} v_{\perp} \left(1 + \frac{\mu}{T} \right)}{1 + q|\nabla h|} \quad \eta = \eta_i.$$

These relations are identified with (4.3) under definition (4.4) for the mobility \mathbf{M} . \square

It can be verified directly that the same limits emerge if the evaluation point of fluxes is at $\eta = \eta_{i+1}$ [28]. Two remarks on results of Proposition 4.1 are in order.

Remark 4.2. In the absence of electromigration ($\mathbf{v} = 0$), we recover the relation $\mathbf{J} = -C_s \mathbf{M} \cdot \nabla \mu$ found previously in [28]. For nonzero drift ($\mathbf{v} \neq 0$), the additional term derived above is affine with μ . This new relation is recast to the zero-drift form via an exponential transformation of μ ; see section 4.4.

Remark 4.3. An alternate proof of Proposition 4.1 makes direct use of the adatom concentration, C_i , and the normal flux component, $J_{i,\perp}$, avoiding entirely the use of integration constants A_i and B_i . This approach treats boundary conditions (3.4) and (3.5) for $\sigma' = \sigma$ as a system of equations for $C_i(\eta_i)$ and $J_{i,\perp}(\eta_i)$. This argument is also applicable to situations where the boundary conditions couple the adatom densities of different terraces, e.g., in the case with step permeability [40]. Details for the present case are presented in Appendix B.

By Proposition 4.1, we state the following corollary for cases of symmetry.

COROLLARY 4.4. *Consider 1D settings with $\mathbf{v} \neq 0$, where translation or rotation symmetry causes all dependent variables to have zero σ -derivatives. The macroscopic*

surface flux corresponding to (4.3) is

$$(4.11) \quad \mathbf{J} = J(\chi)e_\chi, \quad J(\chi) = -\frac{C_s D_s}{T} \frac{\partial_\chi \mu}{1 + q|\partial_\chi h|} + \frac{C_s v}{1 + q|\partial_\chi h|} \left(1 + \frac{\mu}{T}\right),$$

where $\chi = x$ for straight steps and $\chi = r = |\mathbf{r}|$ for concentric circular steps, and $q = 2D_s/(ka)$. Equation (4.11) is in agreement with the 1D limits computed directly in Appendix A for $\tau = \infty$ and discussed in sections 2.1 and 2.2.

Recall that, in the microscale model underlying the limit of this section, the contribution $(\text{div} \mathbf{v})C_i$ is left out from the terrace diffusion equation (see section 2.2). For a discussion on a respective correction to the macroscopic limit, see Remark 5.4.

4.3. Evolution equation in Cartesian system. In this section, we describe the PDE for the surface height by combining ingredients (4.1)–(4.4) and making use of Cartesian coordinates, (x, y) .

First, we introduce the nonsingular orthogonal matrix [28]

$$(4.12) \quad \mathbf{S}(\partial_x h, \partial_y h) = (e_\eta \ e_\sigma) = \frac{1}{|\nabla h|} \begin{pmatrix} -\partial_x h & \partial_y h \\ -\partial_y h & -\partial_x h \end{pmatrix} \quad (\nabla h \neq 0).$$

The mobility tensor \mathbf{M} , which is defined by (4.3) in the (η, σ) coordinate system, is now expressed in the Cartesian coordinate system (x, y) by

$$(4.13) \quad \mathbf{M}_{(x,y)} = S \mathbf{M}_{(\eta,\sigma)} S^T;$$

as usual, S^T denotes the transpose of S ($S^T = S^{-1}$). The Cartesian components of the surface flux (4.3) read (e_l : orthonormal vectors, $l = x, y$):

$$(4.14) \quad J_x = -\frac{C_s}{1 + q|\nabla h|} \left\{ \frac{D_s}{T} \left[\left(1 + q \frac{(\partial_y h)^2}{|\nabla h|}\right) \partial_x \mu - q \frac{(\partial_x h)(\partial_y h)}{|\nabla h|} \partial_y \mu \right] - \left(1 + \frac{\mu}{T}\right) \left[\left(1 + q \frac{(\partial_y h)^2}{|\nabla h|}\right) v_x - q \frac{(\partial_x h)(\partial_y h)}{|\nabla h|} v_y \right] \right\},$$

$$(4.15) \quad J_y = -\frac{C_s}{1 + q|\nabla h|} \left\{ \frac{D_s}{T} \left[\left(1 + q \frac{(\partial_x h)^2}{|\nabla h|}\right) \partial_y \mu - q \frac{(\partial_x h)(\partial_y h)}{|\nabla h|} \partial_x \mu \right] - \left(1 + \frac{\mu}{T}\right) \left[\left(1 + q \frac{(\partial_x h)^2}{|\nabla h|}\right) v_y - q \frac{(\partial_y h)(\partial_x h)}{|\nabla h|} v_x \right] \right\};$$

$$v_l = e_l \cdot \mathbf{v} \quad (l = x, y).$$

The PDE for the surface height follows from the mass conservation statement. Using the Cartesian representation of (4.1), we have

$$(4.16) \quad \partial_t h = -\Omega(\partial_x J_x + \partial_y J_y).$$

This relation leads to a nonlinear, fourth-order parabolic PDE for h after substitution for J_x, J_y , and μ from (4.14), (4.15), and (4.2).

4.4. Change of variables. We show that, if $\text{curl} \mathbf{v} = 0$, (4.3) is recast to

$$(4.17) \quad \mathbf{J} = -c \mathbb{M} \cdot \nabla \vartheta \quad (c = \text{const}),$$

leading to the nondimensional PDE

$$(4.18) \quad \partial_t \tilde{h} = \text{div}^\alpha [\mathbb{M} \cdot \nabla^\alpha \vartheta].$$

We consider an initial height profile with typical amplitude H and lengths λ_x and λ_y in the x and y directions, respectively. Naturally, we scale h by H and the coordinates x, y by λ_x, λ_y . Hence, we make the substitutions $\tilde{h} := h/H$, $\tilde{x} := x/\lambda_x$, $\tilde{y} := y/\lambda_y$ and define $\alpha := \lambda_x/\lambda_y$. With these definitions, the gradient and divergence operators are written as $\nabla = \lambda_x^{-1} \nabla^\alpha$ and $\text{div} = \lambda_x^{-1} \text{div}^\alpha$, where $\nabla^\alpha := (\partial_{\tilde{x}}, \alpha \partial_{\tilde{y}})$ and $\text{div}^\alpha := \partial_{\tilde{x}} + \alpha \partial_{\tilde{y}}$.

The chemical potential (4.2) is scaled by T , $\tilde{\mu} := \mu/T$, and (4.3) reads

$$(4.19) \quad \mathbf{J} = -\frac{C_s D_s}{\lambda_x} \widetilde{\mathbf{M}} \cdot [\nabla^\alpha \tilde{\mu} - \tilde{\mathbf{v}}(1 + \tilde{\mu})],$$

where the mobility $\widetilde{\mathbf{M}}$ —in the (x, y) representation—and drift velocity $\tilde{\mathbf{v}}$ are

$$(4.20) \quad \widetilde{\mathbf{M}}_{(x,y)} := \tilde{\mathbf{S}} \cdot \begin{pmatrix} \frac{1}{1 + \tilde{q} |\nabla^\alpha \tilde{h}|} & 0 \\ 0 & 1 \end{pmatrix} \cdot \tilde{\mathbf{S}}^T, \quad \tilde{\mathbf{v}} := \frac{\lambda_x}{D_s} \mathbf{v}; \quad \tilde{q} := \frac{qH}{\lambda_x}.$$

The corresponding change-of-basis matrix is $\tilde{\mathbf{S}} \equiv \mathbf{S}(\partial_{\tilde{x}} \tilde{h}, \alpha \partial_{\tilde{y}} \tilde{h})$; cf. (4.12).

Consequently, the PDE for the nondimensional height \tilde{h} reads

$$(4.21) \quad \partial_{\tilde{t}} \tilde{h} = \text{div}^\alpha \{ \widetilde{\mathbf{M}} \cdot [\nabla^\alpha \tilde{\mu} - \tilde{\mathbf{v}}(1 + \tilde{\mu})] \}; \quad \tilde{t} := t/t_0, \quad t_0 := \frac{H \lambda_x^2}{\Omega C_s D_s}.$$

To show (4.17) and (4.18), start with the transformation $\vartheta = (1 + \tilde{\mu}) f^\vartheta$. By virtue of $\mathbb{M} \cdot \nabla^\alpha \vartheta = (\mathbb{M} f^\vartheta) \cdot [\nabla^\alpha \tilde{\mu} + (\nabla^\alpha f^\vartheta / f^\vartheta)(1 + \tilde{\mu})]$ and (4.19), we have the consistency relations $\mathbb{M} f^\vartheta = \widetilde{\mathbf{M}}$ and $(\nabla^\alpha f^\vartheta) / f^\vartheta = -\tilde{\mathbf{v}}$. The second one yields

$$f^\vartheta(\tilde{x}, \tilde{y}) = A e^{-\int_0^{(\tilde{x}, \tilde{y}/\alpha)} \tilde{\mathbf{v}}(\mathbf{z}) \cdot d\mathbf{z}} \Rightarrow \mathbb{M} = A^{-1} \widetilde{\mathbf{M}} (\nabla^\alpha \tilde{h}) e^{\int_0^{(\tilde{x}, \tilde{y}/\alpha)} \tilde{\mathbf{v}}(\mathbf{z}) \cdot d\mathbf{z}} \quad (A = \text{const}).$$

Thus,

$$(4.22) \quad \vartheta(\tilde{x}, \tilde{y}) = \left\{ 1 - \tilde{\mu}_0 \text{div}^\alpha \left[\tilde{g} \frac{\nabla^\alpha \tilde{h}}{|\nabla^\alpha \tilde{h}|} + |\nabla^\alpha \tilde{h}| \nabla^\alpha \tilde{h} \right] \right\} e^{-\int_0^{(\tilde{x}, \tilde{y}/\alpha)} \tilde{\mathbf{v}}(\mathbf{z}) \cdot d\mathbf{z}}.$$

5. Extensions of macroscopic limit. In an attempt to formulate a reasonably general theory of macroscopic surface relaxation, we enrich the BCF model with additional microscale effects. These are the following: (i) the exponential law $C_i^{\text{eq}} = C_s \exp(\mu_i/T)$ in the place of its linearization; (ii) atom desorption; and (iii) anisotropic terrace diffusion and step edge atom diffusion [39]. Our broader goal with these extensions is to reconcile the macroscopic theory with realistic situations where an electric field is present. We show that (i) and (iii) can modify significantly the constitutive relation between surface flux and chemical potential. In contrast, effect (ii) arguably has vanishingly small influence on the macroscopic evolution law.

5.1. Exponential law for step chemical potential. To derive the constitutive relation between large-scale flux and chemical potential, we approximated the difference of equilibrium concentrations C_i^{eq} by use of the linearized form (2.4). The quantitative justification for this approximation is not clear in the literature, particularly since the chemical potential μ_i is not measured directly.¹² However, the

¹²It should be borne in mind that the linearization of C_i^{eq} with μ_i has been used widely in comparisons of theoretical results and experimental data and seems to work reasonably well [16].

PDE is easily modified to accommodate the complete, exponential law. For a similar modification in 1+1 dimensions with $v = 0$ and long-range step interactions, see [56].

By skipping details irrelevant to the modification at hand, we start from (4.8). By setting $\mu_i = \mu(\mathbf{r})|_{\eta_i}$ we expand the difference $C_{i+1}^{\text{eq}} - C_i^{\text{eq}}$ as follows:

$$\begin{aligned} C_{i+1}^{\text{eq}} - C_i^{\text{eq}} &= C_s \left[\exp\left(\frac{\mu_{i+1}}{T}\right) - \exp\left(\frac{\mu_i}{T}\right) \right] \\ &= \frac{aC_s}{|\nabla h|} \exp\left(\frac{\mu(\tilde{\eta})}{T}\right) \frac{\partial_{\perp} \mu(\tilde{\eta})}{T}, \quad \tilde{\eta} \in [\eta_i, \eta_{i+1}]. \end{aligned}$$

Hence, the normal flux component $J_{i,\perp}$ at (η_i, σ) becomes

$$(5.1) \quad J_{i,\perp}|_{\eta_i} = \frac{-\frac{D_s}{\xi_{\eta} \delta \eta_i} \frac{aC_s}{|\nabla h|} \exp\left(\frac{\mu(\tilde{\eta})}{T}\right) \frac{\partial_{\perp} \mu(\tilde{\eta})}{T} + v_{\perp} C_s \exp\left(\frac{\mu(\eta_i)}{T}\right)}{\frac{D_s}{\xi_{\eta} \delta \eta_i} \left(\frac{1}{k_u} + \frac{1}{k_d}\right) + \left(1 + \frac{v_{\perp}}{k_u}\right)}.$$

Similarly, the σ -derivative of C_i^{eq} appearing in (4.7) for the longitudinal flux component, $J_{i,\parallel}$, now acquires exponential factors when expressed in terms of μ_i :

$$(5.2) \quad \begin{aligned} J_{i,\parallel}|_i &= \left[-\frac{D_s}{\xi_{\eta} \delta \eta_i} \left(\frac{1}{k_u} + \frac{1}{k_d}\right) - 1 \right]^{-1} \left\{ -\frac{C_s D_s}{\xi_{\eta} \delta \eta_i} v_{\parallel} \left[\frac{1}{k_d} \exp\left(\frac{\mu_i}{T}\right) + \frac{1}{k_u} \exp\left(\frac{\mu_{i+1}}{T}\right) \right] \right. \\ &\quad - v_{\parallel} C_s \exp\left(\frac{\mu_i}{T}\right) + D_s C_s \exp\left(\frac{\mu_i}{T}\right) \frac{\partial_{\parallel} \mu_i}{T} \\ &\quad + \frac{D_s^2 C_s}{k_d \xi_{\eta} \delta \eta_i} \exp\left(\frac{\mu_i}{T}\right) \frac{\partial_{\parallel} \mu_i}{T} \\ &\quad \left. + \frac{D_s^2 C_s}{k_u \xi_{\eta} \delta \eta_i} \exp\left(\frac{\mu_{i+1}}{T}\right) \frac{\partial_{\parallel} \mu_{i+1}}{T} \right\}. \end{aligned}$$

The coarse-graining procedure carries through as in Proposition 4.1. The components of the flux $\mathbf{J}(\mathbf{r})$ are found to satisfy the equations

$$(5.3) \quad J_{\perp}(\mathbf{r}) \left(\frac{2}{k} + \frac{a}{D_s |\nabla h|} \right) = \exp\left[\frac{\mu(\mathbf{r})}{T}\right] \left\{ -\frac{aC_s}{|\nabla h|} \frac{\partial_{\perp} \mu(\mathbf{r})}{T} + v_{\perp} \frac{aC_s}{D_s |\nabla h|} \right\},$$

$$(5.4) \quad C_s \exp\left[\frac{\mu(\mathbf{r})}{T}\right] \frac{\partial_{\parallel} \mu(\mathbf{r})}{T} = -\frac{1}{D_s} \left\{ J_{\parallel}(\mathbf{r}) - v_{\parallel} C_s \exp\left[\frac{\mu(\mathbf{r})}{T}\right] \right\}.$$

The last two equations result in the effective constitutive relation (1.2).

By inspection of (1.2), we have the following remark.

Remark 5.1. For $\text{curl} \mathbf{v} = 0$, the modified constitutive relation for the macroscopic flux results from the invariant under the law $C^{\text{eq}} = C^{\text{eq}}[\mu]$ form (4.18) and

$$(5.5) \quad \vartheta(\mathbf{r}) := e^{\mu(\mathbf{r})/T - D_s^{-1} \int_0^{\mathbf{r}} \mathbf{v}(\mathbf{z}) \cdot d\mathbf{z}},$$

which is a direct extension of the linearized version, (4.22).

5.2. Adatom desorption. The effect of desorption is expected to affect only the relation between the large-scale surface flux and chemical potential. In this section, we show that, under certain conditions, desorption does not appear in the macroscopic laws to leading order in a . Corrections due to desorption in Fick’s law for the macroscale flux are computed and discussed.

5.2.1. Solution for microscale diffusion. Following the rationale of slow and fast step variables of section 3.3, we write the (quasi-steady) diffusion equation on the i th terrace with desorption time τ and a drift velocity \mathbf{v} ($v_{\perp} = e_{\eta} \cdot \mathbf{v}$) as

$$(5.6) \quad \partial_{\eta} \left(\frac{\xi_{\sigma}}{\xi_{\eta}} \partial_{\eta} C_i \right) - \frac{v_{\perp} \xi_{\sigma}}{D_s} \partial_{\eta} C_i \sim \frac{\xi_{\eta} \xi_{\sigma}}{\tau D_s} C_i \quad (\eta_i < \eta < \eta_{i+1}).$$

A first observation is that, for $v_{\perp} \neq 0$ and $\tau \neq \infty$, this equation does not admit a relatively simple solution, i.e., in terms of elementary functions. (The radial case of section 2.2 certainly alludes to the same conclusion.)

It is of interest to note that there are at least two ways of solving (5.6). First, it can be converted to a canonical ordinary differential equation (ODE) solvable by confluent hypergeometric functions [7]. This route is not particularly informative. Alternatively, (5.6) can be recast to a Volterra integral equation, which can be solved by iterations through a (convergent) Born–Neumann series [53].

We now focus on the (simpler) integral-equation formulation for (5.6).¹³

PROPOSITION 5.2. *Suppose C_i is a solution of the PDE (5.6). Then C_i satisfies the following Volterra equation on $\eta_i < \eta < \eta_{i+1}$:*

$$(5.7) \quad C_i(\eta, \sigma) = [B_i(\sigma) + A_i(\sigma) f_i(\eta, \sigma)] + [u_{i,1}(\eta, \sigma) + u_{i,2}(\eta, \sigma) f_i(\eta, \sigma)],$$

where

$$(5.8) \quad u_{i,1}(\eta, \sigma) = u_{i,1}[C_i] = -(\tau D_s)^{-1} \int_{\eta_i}^{\eta} \frac{f_i(\eta', \sigma) \xi_{\eta'}^2 C_i(\eta', \sigma)}{\mathcal{W}(\eta')} d\eta',$$

$$(5.9) \quad u_{i,2}(\eta, \sigma) = u_{i,2}[C_i] = (\tau D_s)^{-1} \int_{\eta_i}^{\eta} \frac{\xi_{\eta'}^2 C_i(\eta', \sigma)}{\mathcal{W}(\eta')} d\eta',$$

$$(5.10) \quad \mathcal{W}(\eta) = \partial_{\eta} f_i = \frac{\xi_{\eta}}{\xi_{\sigma}} \exp \left[D_s^{-1} \int_{\eta_i}^{\eta} \xi_{\eta'} (v_{\perp} |_{\eta'}) d\eta' \right],$$

$f_i(\eta, \sigma)$ is defined by (3.13), and the coefficients $A_i(\sigma)$ and $B_i(\sigma)$ are determined through boundary conditions (3.4) and (3.5) for atom attachment-detachment at $\eta = \eta_i, \eta_{i+1}$. Note that $\mathcal{W}(\eta)$ is the Wronskian of the two homogeneous (for $\tau = \infty$) solutions of ODE (5.6), namely, the functions 1 and $f_i(\eta, \cdot)$.

Proof. We provide a sketch of the proof since this relies on standard techniques for linear ODEs and PDEs. Consider the (τ -dependent) term in the right-hand side of (5.6) as a forcing. Apply Duhamel’s principle (or the method of “variation of parameters”) to construct a particular solution of the ODE. This approach yields C_i as a sum of the following: (i) a linear combination of the two homogeneous solutions, 1 and f_i ; and (ii) a τ^{-1} -scaled particular solution, which involves two distinct integrals of C_i/τ (one for each homogeneous solution). The coefficients A_i and B_i in the aforementioned linear combination are determined via enforcement of the boundary conditions. \square

Integral equation (5.7) can be solved by the conventional iteration (Born–Neumann) scheme [53]: First, set $C_i = 0$ under the integral (in $u_{i,1}$ and $u_{i,2}$) and obtain $C_i \sim B_i + A_i f_i$; second, replace C_i by $B_i + A_i f_i$ under the integral; next, repeat successively with the updated C_i . Because the kernel is L^2 and smooth, the series generated by iterations converges to the solution C_i for all $\tau > 0$ and yields a smooth C_i . Since the kernel is proportional to τ^{-1} , the procedure yields a power series in $1/\tau$, whose convergence is thus enhanced by increasing τ .

¹³For notational simplicity, we use σ in the place of the slow variable $\tilde{\sigma}$.

The importance of the Born–Neumann scheme becomes evident for $\eta - \eta_i \ll 1$. Since $\int_{\eta_i}^{\eta} F(\eta') \, d\eta' = F(\eta_i)(\eta - \eta_i) + o(\eta - \eta_i)$ for any continuous F , the associated iterated integrals contribute respective ascending powers of $\eta - \eta_i$. So, evidently, in the limit $\max_i \{\delta\eta_i\} = \max_i \{\eta_{i+1} - \eta_i\} \downarrow 0$, constructing a solution to (5.7) via a Born–Neumann series corresponds to producing a Taylor series in $\eta - \eta_i$ for $C_i(\eta, \sigma)$. This result is directly applicable to the macroscopic limit of the step system.

5.2.2. Limit $a \downarrow 0$. Next, we derive a macroscopic Fick’s law with desorption and external electric field. We follow the main procedure of Proposition 4.1 by use of formula (5.7) (in Proposition 5.2) for C_i . Suppressing the σ dependence, we define

$$(5.11) \quad C_i^v(\eta) := B_i + A_i f_i(\eta),$$

which is the solution *form* without desorption.¹⁴ Thus, C_i satisfies

$$(5.12) \quad C_i(\eta) - C_i^v(\eta) = (\tau D_s)^{-1} \int_{\eta_i}^{\eta} \xi_{\eta'}^2 \frac{f_i(\eta) - f_i(\eta')}{\partial_{\eta'} f_i} C_i(\eta') \, d\eta'.$$

By differentiation of (5.12) with respect to η we obtain the normal flux component, $J_{i,\perp} = e_{\eta} \cdot (-D_s \nabla C_i + \mathbf{v} C_i)$:

$$(5.13) \quad J_{i,\perp} - J_{i,\perp}^v = -\frac{\partial_{\perp} f_i}{\tau} \int_{\eta_i}^{\eta} \frac{\xi_{\eta'}^2 C_i(\eta')}{\partial_{\eta'} f_i} \, d\eta' + \frac{v_{\perp}}{\tau D_s} \int_{\eta_i}^{\eta} \xi_{\eta'}^2 \frac{f_i(\eta) - f_i(\eta')}{\partial_{\eta'} f_i} C_i(\eta') \, d\eta',$$

where $J_{i,\perp}^v := -D_s \partial_{\perp} C_i^v + v_{\perp} C_i^v$; recall that $\partial_{\perp} = \xi_{\eta}^{-1} \partial_{\eta}$.

Now consider the limit $\delta\eta := \eta - \eta_i \downarrow 0$. By Taylor expanding the right-hand sides of (5.12) and (5.13), we readily obtain

$$(5.14) \quad C_i(\eta) - C_i^v(\eta) = (2D_s \tau)^{-1} C_i^v(\eta_i) \xi_{\eta_i}^2 \delta\eta^2 + \mathcal{O}(\delta\eta^3),$$

$$(5.15) \quad J_{i,\perp}(\eta) - J_{i,\perp}^v(\eta) = -\tau^{-1} C_i^v(\eta_i) \xi_{\eta_i} \delta\eta + \mathcal{O}(\delta\eta^2) \quad \text{as } \delta\eta \downarrow 0.$$

Next, we apply conditions (3.4) and (3.5) for $\sigma' = \sigma$. With recourse to $C_i^v(\eta_{i+1}) = C_i^v(\eta_i) + (\partial_{\eta} C_i^v)|_{\eta_i} \delta\eta_i + o(\delta\eta_i)$, and likewise for $J_{i,\perp}(\eta_{i+1})$, we find

$$(5.16) \quad -k_u^{-1} J_{i,\perp}^v = C_i^v - C_i^{\text{eq}},$$

$$(5.17) \quad k_d^{-1} \left[\left(1 + \frac{k_d}{D_s} \delta w_i \right) J_{i,\perp}^v + (\partial_{\perp} J_{i,\perp}^v) \delta w_i \right] \sim \left[1 + \left(\frac{v_{\perp}}{D_s} + \frac{1}{k_d \tau} + \frac{\delta w_i}{2D_s \tau} \right) \delta w_i \right] C_i^v - C_{i+1}^{\text{eq}},$$

where $\delta w_i := \xi_{\eta_i} \delta\eta_i$, and C_i^v , $J_{i,\perp}^v$, and $\partial_{\perp} J_{i,\perp}^v$ are evaluated at η_i . Note that (5.16) does not involve τ explicitly. In contrast, (5.17) manifests desorption terms in the right-hand side. If these, τ^{-1} -scaled, terms can be neglected appropriately, the resulting system becomes identical to that without desorption; the corresponding terms in C_i and $J_{i,\perp}$ can then be dropped.

Remark 5.3. By inspection of the (attachment-detachment) boundary conditions (5.16) and (5.17) for the adatom flux and density, sufficient conditions for neglecting the desorption effect in the macroscopic limit (assuming $k/k_{\ell} = \mathcal{O}(1)$, $\ell = u, d$) are

$$(5.18) \quad \frac{|\mathbf{v}|}{D_s} \gg \frac{1}{k\tau} \quad \text{and} \quad |\mathbf{v}| \ll k.$$

¹⁴ A_i and B_i entering C_i^v in principle depend on τ via boundary conditions at step edges.

Then, the large-scale adatom flux is not affected by τ uniformly in space coordinates. In particular, the first condition amounts to having $|\mathbf{v}|\tau \gg a$ and thus $a \ll k\tau$ when $D_s/(ka) = \mathcal{O}(1)$. These conditions are expected to be met in a wide range of physical situations; see, e.g., [4]. From the viewpoint of coarse graining and perturbation theory, (5.18) simply state that the effect of desorption is of higher order (in a).

Interestingly, by keeping desorption terms, thus relaxing conditions (5.18) perhaps naively, we acquire a macroscopic flux that is asymmetric in k_u and k_d . We proceed to assert this claim. Let us consider attachment-detachment limited kinetics, $k\delta w_i/D_s \ll 1$ (δw_i : i th terrace width), under $|\mathbf{v}|/k \ll 1$. By (3.4) and (3.5), A_i and B_i satisfy

$$-\frac{D_s}{\xi_\sigma k_u} A_i + \left(1 + \frac{v_\perp}{k_u}\right) B_i = C_i^{\text{eq}},$$

$$\left[\frac{D_s}{\xi_\sigma k_d} + \left(1 - \frac{v_\perp}{k_d}\right) \frac{\delta w_i}{\xi_\sigma}\right] A_i + \left(1 - \frac{v_\perp}{k_d} + \frac{\delta w_i}{k_d \tau}\right) B_i = C_{i+1}^{\text{eq}},$$

with solution

$$(5.19) \quad A_i = \xi_\sigma \frac{-C_i^{\text{eq}} \left(1 - \frac{v_\perp}{k_d} + \frac{\delta w_i}{k_d \tau}\right) + C_{i+1}^{\text{eq}} \left(1 + \frac{v_\perp}{k_u}\right)}{D_s \left(\frac{1}{k_u} + \frac{1}{k_d}\right) + \delta w_i + \frac{D_s}{k_u} \frac{\delta w_i}{k_d \tau}},$$

$$(5.20) \quad B_i = \frac{\frac{D_s}{k_u} C_{i+1}^{\text{eq}} + \left[\frac{D_s}{k_d} + \left(1 - \frac{v_\perp}{k_d}\right) \delta w_i\right] C_i^{\text{eq}}}{D_s \left(\frac{1}{k_u} + \frac{1}{k_d}\right) + \delta w_i + \frac{D_s}{k_u} \frac{\delta w_i}{k_d \tau}}.$$

After some algebra, the normal flux component at $\eta = \eta_i$ is

$$(5.21) \quad J_{i,\perp}(\eta_i) \sim -D_s \frac{\frac{C_{i+1}^{\text{eq}} - C_i^{\text{eq}}}{\delta w_i} - \left(\frac{v_\perp}{D_s} + \frac{1}{k_d \tau}\right) C_i^{\text{eq}}}{\frac{2D_s}{k \delta w_i} + \frac{D_s}{k_u k_d \tau}} \xrightarrow{a \downarrow 0} -(ka) \frac{\partial_\perp - \left(\frac{v_\perp}{D_s} + \frac{1}{k_d \tau}\right)}{|\nabla h| + \frac{a}{(k_u + k_d)\tau}} C^{\text{eq}},$$

i.e., with a term in the numerator that singles out the down-step kinetic rate, k_d . Our computation suggests that the τ -dependent corrections for the normal flux might not be trusted as they appear too sensitive to microstructure details.

With no restriction on $D_s/(k_\ell a)$, the normal flux component is

$$(5.22) \quad J_{i,\perp} \xrightarrow{a \downarrow 0} J_\perp = -D_s \frac{\partial_\perp - \frac{v_\perp}{D_s} - (1 + q_d |\nabla h|) \frac{1}{2D_s \tau} \frac{a}{|\nabla h|}}{1 + q \left(|\nabla h| + \frac{a}{(k_u + k_d)\tau}\right) + \frac{1}{k\tau} \frac{a}{|\nabla h|}} C^{\text{eq}}; \quad q_d := \frac{2D_s}{k_d a}.$$

The corresponding parallel flux component reads

$$J_{i,\parallel}(\eta_i) \xrightarrow{a \downarrow 0} J_\parallel = \frac{1 + q |\nabla h|}{1 + q \left(|\nabla h| + \frac{a}{(k_u + k_d)\tau}\right) + \frac{1}{k\tau} \frac{a}{|\nabla h|}} (-D_s \partial_\parallel + v_\parallel) C^{\text{eq}},$$

which, in contrast to J_\perp , is symmetric in k_u and k_d ; cf. (4.3) and (4.4) with $C^{\text{eq}} \sim C_s(1 + \mu/T)$.

We conclude this section with the following observation.

Remark 5.4. The (thus far neglected) term $(\text{div}\mathbf{v})C_i$ in the terrace diffusion equation for the adatom density C_i can be treated on the same footing as the desorption term C_i/τ . Hence, in assessing the validity of dropping the former, it is reasonable to repeat the above procedure with τ^{-1} being replaced by $\text{div}\mathbf{v}$, in an appropriate sense.

5.3. Anisotropic terrace diffusion and edge atom diffusion. We now invoke the methodology of [39] to provide an extended formula for the macroscopic surface flux \mathbf{J} . At the microscale (BCF level), we consider anisotropic diffusion of adatoms, i.e., a *tensor* diffusivity \mathbf{D}_s , and edge atom diffusion with coefficient D_e .

The mass conservation statement now reads [39]

$$(5.23) \quad v_i = e_\eta \cdot \frac{d\mathbf{r}_i}{dt} = \frac{\Omega}{a}(J_{i-1,\perp}^{tr} - J_{i,\perp}^{tr}) + a\partial_s \left(D_e \frac{\partial_{\parallel}\mu_i}{T} \right) \quad \eta = \eta_i,$$

where $J_{i,\perp}^{tr} = e_\eta \cdot \mathbf{J}_i^{tr}$, \mathbf{J}_i^{tr} is the flux of *terrace* adatoms, and the last term in (5.23) describes diffusion along the step edge leaving out the electric-field drift of edge atoms. The microscale diffusion equation (in the quasi-steady approximation) has the form

$$(5.24) \quad -\text{div}(\mathbf{D}_s \cdot \nabla C_i) + \mathbf{v} \cdot \nabla C_i = 0 \quad \eta_i < \eta < \eta_{i+1},$$

still assuming that $|(\text{div}\mathbf{v})C_i| \ll |\mathbf{v} \cdot \nabla C_i|$, where the drift velocity is $\mathbf{v} = Z^* e \mathbf{D}_s \cdot \mathbf{E}/T$. In the (η, σ) representation the (positive-definite) coefficient \mathbf{D}_s is written as

$$(5.25) \quad \mathbf{D}_s = D_{11}e_\eta e_\eta + D_{12}e_\eta e_\sigma + D_{21}e_\sigma e_\eta + D_{22}e_\sigma e_\sigma := \begin{pmatrix} D_{11} & D_{12} \\ D_{21} & D_{22} \end{pmatrix};$$

we have $\det(\mathbf{D}_s) = D_{11}D_{22} - D_{12}D_{21} > 0$. The form of attachment-detachment boundary conditions (3.4) and (3.5) remains intact.

Next, we derive a relation between the large-scale terrace adatom flux, \mathbf{J}^{tr} , and the chemical potential gradient, $\nabla\mu$. For simplicity, we adopt the procedure of Taylor expansions from [39], which has the flavor of the derivation in Appendix B. First, we invert the microscale relation $\mathbf{J}_i^{tr} - \mathbf{v}C_i = -\mathbf{D}_s \cdot \nabla C_i$ to obtain the partial derivatives of C_i in terms of $(J_{i,\perp}^{tr}, J_{i,\parallel}^{tr})$ and C_i :

$$(5.26) \quad \begin{pmatrix} \xi_\eta^{-1} \partial_\eta C_i \\ \xi_\sigma^{-1} \partial_\sigma C_i \end{pmatrix} = - \begin{pmatrix} D_{11} & D_{12} \\ D_{21} & D_{22} \end{pmatrix}^{-1} \cdot \begin{pmatrix} J_{i,\perp}^{tr} - v_\perp C_i \\ J_{i,\parallel}^{tr} - v_\parallel C_i \end{pmatrix} \\ = \frac{1}{|\mathbf{D}_s|} \begin{pmatrix} -D_{22}J_{i,\perp}^{tr} + D_{12}J_{i,\parallel}^{tr} + (v_\perp D_{22} - v_\parallel D_{12})C_i \\ D_{21}J_{i,\perp}^{tr} - D_{11}J_{i,\parallel}^{tr} - (v_\perp D_{21} - v_\parallel D_{11})C_i \end{pmatrix}; \quad |\mathbf{D}_s| := \det(\mathbf{D}_s).$$

Second, we resort to (3.4) and (3.5) with $\sigma' = \sigma + \delta\sigma$: By Taylor-expanding $J_{i,\perp}^{tr}(\eta_{i+1})$ and $C_i(\eta_{i+1})$ at (η_i, σ) and dropping derivatives of $J_{i,\perp}^{tr}$,¹⁵ we have

$$(5.27) \quad \begin{aligned} -k_u^{-1} J_{i,\perp}^{tr} &= C_i - C_i^{\text{eq}}, \\ -k_d^{-1} J_{i,\perp}^{tr} &= C_i + \delta\eta_i \partial_\eta C_i + \delta\sigma \partial_\sigma C_i - C_{i+1}^{\text{eq}} \quad \text{at } (\eta_i, \sigma). \end{aligned}$$

¹⁵This approximation can be justified a posteriori and is consistent with independently derived results for the following: (i) $\mathbf{v} = 0$ and tensorial \mathbf{D}_s ; and (ii) $\mathbf{v} \neq 0$ and scalar \mathbf{D}_s .

In view of (5.26), replace $(\partial_\eta C_i, \partial_\sigma C_i)$ in terms of $(J_{i,\perp}^{tr}, J_{i,\parallel}^{tr})$ and C_i , and set $C_i^{\text{eq}} = C^{\text{eq}}(\mathbf{r})|_{\eta_i}$ for smooth $C^{\text{eq}}(\mathbf{r})$. By adding equations (5.27), we conclude by dominant balance that $C_i \sim C^{\text{eq}}|_{\eta_i}$ as $\delta\eta_i \downarrow 0$ (see also [40]); by subtracting we have

$$(5.28) \quad \begin{aligned} |\mathbf{D}_s|(k_d^{-1} + k_u^{-1})J_\perp^{tr} &= \delta w[(v_\perp D_{22} - v_\parallel D_{12})C^{\text{eq}} + (-D_{22}J_\perp^{tr} + D_{12}J_\parallel^{tr}) - |\mathbf{D}_s|\partial_\perp C^{\text{eq}}] \\ &+ \delta s[(v_\parallel D_{11} - v_\perp D_{21})C^{\text{eq}} + (D_{21}J_\perp^{tr} - D_{11}J_\parallel^{tr}) - |\mathbf{D}_s|\partial_\parallel C^{\text{eq}}], \end{aligned}$$

where $\delta w \equiv \delta w_i = \xi_\eta^{-1} \delta\eta_i \sim a/(|\nabla h|)|_{\eta_i}$ and $\delta s = \xi_\sigma^{-1} \delta\sigma$ (i th-step edge infinitesimal arc length). Thus, we obtain the following relations for $(J_\perp^{tr}, J_\parallel^{tr})$:

$$(5.29) \quad \begin{aligned} \left(\frac{2|\mathbf{D}_s|}{ka} |\nabla h| + D_{22} \right) J_\perp^{tr} - D_{12} J_\parallel^{tr} &= -|\mathbf{D}_s| \partial_\perp C^{\text{eq}} + (v_\perp D_{22} - v_\parallel D_{12}) C^{\text{eq}}, \\ D_{21} J_\perp^{tr} - D_{11} J_\parallel^{tr} &= |\mathbf{D}_s| \partial_\parallel C^{\text{eq}} + (v_\perp D_{21} - v_\parallel D_{11}) C^{\text{eq}}. \end{aligned}$$

Solving this system for $(J_\perp^{tr}, J_\parallel^{tr})$ yields

$$(5.30) \quad \begin{aligned} \begin{pmatrix} J_\perp^{tr} \\ J_\parallel^{tr} \end{pmatrix} &= (1 + q|\nabla h|)^{-1} \left[- \begin{pmatrix} D_{11} & D_{12} \\ D_{21} & D_{22} + \mathcal{D}^{tr} |\nabla h| \end{pmatrix} \cdot \begin{pmatrix} \partial_\perp C^{\text{eq}} \\ \partial_\parallel C^{\text{eq}} \end{pmatrix} \right. \\ &\quad \left. + \begin{pmatrix} 1 & 0 \\ -\frac{2D_{21}}{ka} |\nabla h| & 1 + q|\nabla h| \end{pmatrix} \cdot \begin{pmatrix} v_\perp \\ v_\parallel \end{pmatrix} C^{\text{eq}} \right]; \\ q &:= \frac{2D_{11}}{ka}, \quad \mathcal{D}^{tr} := \frac{2|\mathbf{D}_s|}{ka}. \end{aligned}$$

This relation is recast to the familiar form

$$(5.31) \quad \mathbf{J}^{tr} = -C_s \mathbf{M}^{tr} \cdot \left[\nabla \mu - T \mathbf{D}_s^{-1} \cdot \mathbf{v} \left(1 + \frac{\mu}{T} \right) \right],$$

which is a direct generalization of (4.3); the adatom mobility \mathbf{M}^{tr} is defined by [39]

$$(5.32) \quad \mathbf{M}^{tr} := \frac{1}{T} \frac{1}{1 + q|\nabla h|} \begin{pmatrix} D_{11} & D_{12} \\ D_{21} & D_{22} + \mathcal{D}^{tr} |\nabla h| \end{pmatrix}.$$

The *total* surface flux is $\mathbf{J} = \mathbf{J}^{tr} + \mathbf{J}^e$ where \mathbf{J}^e is the contribution of edge atoms by the step velocity law (5.23). From [39] we have the conservation law $\partial_t h + \Omega \text{div}(\mathbf{J}^{tr} + \mathbf{J}^e) = 0$ where

$$(5.33) \quad \mathbf{J}^e = J_\parallel^e e_\sigma, \quad J_\parallel^e = -\frac{aD_e}{T\Omega} |\nabla h| \partial_\parallel \mu.$$

6. Discussion. In this section we discuss from a macroscopic perspective the possibility of manipulating the surface morphology by use of an electric field. First, we review and discuss the onset of step bunching instabilities in straight-step and axisymmetric settings. Second, we capture *stationary* properties of PDE solutions for h near the edge of a facet (where $\nabla h = 0$), avoiding pending issues related to the coupling of the PDE (outside the facet) with the microscale step motion on top of the facet [27]. We only enforce slope continuity, thus requiring that the slope profile approaches zero near the facet edge.

6.1. On bunching instabilities. In this subsection, we review from a PDE perspective bunching instabilities in 1D, i.e., for straight and circular steps (see Corollary 4.4). Within full continuum, such instabilities arise through backward-diffusion terms in the parabolic PDE for h . For related works, see, e.g., the reviews by Krug [17, 18] and references therein. In particular, we indicate the plausible use of an electric field for manipulation of bunching phenomena where the step curvature can be important.

In the following (for this subsection) we use $1 + \mu/T \approx 1$ when possible. We consider attachment-detachment limited kinetics, assuming that the slope $m = |\nabla h|$ and kinetic parameter $q = 2D_s/(ka)$ (k : harmonic average of k_u, k_d) satisfy the condition $qm \gg 1$. (Facets, where $m = 0$, are precluded.)

6.1.1. Straight steps revisited. Consider a monotonic step train where $\partial_x h < 0$. With recourse to the 1D version of (1.3) (see Corollary 4.4), the (x -directed) flux and chemical potential read

$$J(x) = \frac{kaC_s}{2T} (\partial_x h)^{-1} \left(\partial_x \mu - \frac{T}{D_s} v \right),$$

$$\mu(x) = \hat{g}_3 \partial_x [(\partial_x h)^2], \quad \partial_x h < 0, \quad \hat{g}_3 := g_3 \Omega.$$

The formula for $J(x)$ stems from coarse graining the step flow model described in section 2.1.1; see Appendix A. By comparison to (4.2), note that the step line tension (g_1 term) does not contribute to $\mu(x)$ since $\text{div}(\nabla h/|\nabla h|) \equiv 0$ in this 1D setting. The PDE for h is

$$(6.1) \quad \partial_t h = -\Omega \partial_x J = \frac{\Omega ka C_s}{2T} \partial_x \left\{ \hat{g}_3 |\partial_x h|^{-1} \partial_x^2 [(\partial_x h)^2] + \frac{T}{D_s} (\partial_x h)^{-1} v \right\}.$$

Remark 6.1. Consider positive material parameter k ($k > 0$) and negative slope $\partial_x h < 0$. If $v > 0$, the drift velocity contributes a backward-diffusion term in (6.1) and thus tends to destabilize surface motion; if $v < 0$, the drift velocity has a stabilizing effect. In contrast, the effect of repulsive step interactions (g_3 term with $g_3 > 0$) is always stabilizing, since it amounts to a forward, fourth-order diffusion term.

This conclusion has been further quantified by linearization of PDE (6.1) around its (trivial) solution $\partial_x h = \text{const}$ [11] and is consistent with well-documented stability analysis of the step model, carried out, e.g., in [4, 51]. Note that the stability effect of v is *reversed* by the change of sign for k . This notion is introduced in [57] and is placed within a macroscopic perspective in [24].

6.1.2. Radial case. It is known [11] that step curvature in the radial setting, without an electric field, can cause bunching analogous to that from an electric field in straight-step geometries. In hindsight, this is not surprising: the curvature-induced step chemical potential gradient in the axisymmetric case creates a surface flux analogous to the electric-field drift in (1+1)-dimensional morphologies. In this subsection, we discuss the plausible joint effect of an electric field and step curvature in axisymmetric morphologies. Then we describe from a macroscopic view how a (step-up) electric force can possibly be tuned to cancel the destabilizing effect of curvature.

The radial surface flux and step chemical potential read

$$J(r) = \frac{kaC_s}{2T} (\partial_r h)^{-1} \left[\partial_r \mu - \frac{T}{D_s} v(r) \right],$$

$$\mu(r) = \frac{\hat{g}_1}{r} + \frac{\hat{g}_3}{r} \partial_r [r(\partial_r h)^2]; \quad \hat{g}_1 := \Omega g_1 > 0, \quad \partial_r h < 0.$$

Thus, the PDE for the positive surface slope, $m = |\partial_r h|$, is

$$(6.2) \quad \partial_t m = \frac{\Omega k a C_s}{2T} \partial_r \left(r^{-1} \partial_r \left[m^{-1} \left\{ \frac{\hat{g}_1}{r} - r \hat{g}_3 \partial_r [r^{-1} \partial_r (r m^2)] + \frac{T}{D_s} r v(r) \right\} \right] \right).$$

First, we state some results concerning instabilities by inspection of (6.2).

Remark 6.2. Consider $k > 0$ and $\partial_r h < 0$. The step curvature term \hat{g}_1/r contributes a backward-diffusion effect in PDE (6.2), which tends to destabilize an axisymmetric step train. In contrast, repulsive step interactions ($\hat{g}_3 > 0$) are stabilizing. The effect of the electric field depends on the sign of v (similar to straight steps): If $v > 0$, the drift is destabilizing; if $v < 0$, the drift is stabilizing.

Next, we address the plausibility of adjusting the electric field so that it suppresses the destabilizing effect of step curvature. By (6.2), a condition for cancellation of step curvature and electromigration effects in the PDE is

$$(6.3) \quad \hat{g}_1 + \frac{T}{D_s} r^2 v(r) = (\mathcal{K}_1 r^2 + \mathcal{K}_2) r m,$$

where \mathcal{K}_1 and \mathcal{K}_2 are reasonably arbitrary integration constants (which may depend on time t). In particular, for $\mathcal{K}_1 = \mathcal{K}_2 = 0$ condition (6.3) amounts to cancellation of the corresponding surface fluxes if $v(r) = v_c(r) := -(D_s/T) g_1 r^{-2}$. In this case, for a monotonically descending step train ($\partial_r h < 0$), condition (6.3) suggests the possible suppression of the curvature effect provided the drift velocity points in the step-up direction and has magnitude $|v| \geq |v_c|$. The condition on v can be improved by including in the electromigration part of J the μ/T term; then, v has to be adjusted spatiotemporally to a correction depending on the slope profile m .

There are various limitations of our approach here. First, at the risk of redundancy, we stress that the experimental significance of the present radial setting has yet to be assessed. Second, even if such a radial setting is feasible, tuning $v(r)$ as dictated by (6.3) (or, its variants via improvements of J) may turn out to be impractical. Third, carrying out the extension of these considerations to full 2D geometries is not thoroughly resolved as yet, even for the case with $\mathbf{v} = 0$. Last, we have not discussed the combined effect of step-step interactions with drift and curvature.

6.2. Slope profile near facet. Next, we address the *singular* behavior of $m = |\nabla h|$ at the edge of a facet (where $\nabla h = 0$), assuming that $m \uparrow 0$ as \mathbf{r} approaches the facet boundary from the sloping surface. We focus on 1D profiles; the extension to full 2D is also discussed. We work with convenient units where $D_s C_s / T = 1$ and restrict attention to diffusion-limited kinetics, i.e., take $q|\nabla h| \ll 1$; so, $1 + q|\nabla h| \sim 1$.

6.2.1. Straight-step morphology. We consider the continuous graph $y = h(x)$ with the facet $\{(x, y) \in \mathbb{R}^2 \mid h = \text{const}\}$ in $x \leq 0$, while $\partial_x h < 0$ in $x > 0$; so the facet edge is at $x = 0$. Setting $\partial_t h \equiv 0$ in the conservation law $\partial_t h + \Omega \partial_x J = 0$, where $J = -[\partial_x \mu - D_s^{-1} v T (1 + \mu/T)]$ entails the ODE

$$(6.4) \quad \partial_x \mu - l_v^{-1} \mu = l_v^{-1} T - \mathcal{J}_0 \Rightarrow \mu(x) = (\mu_0 + T - l_v \mathcal{J}_0) e^{x/l_v} - (T - l_v \mathcal{J}_0) \quad x > 0;$$

here, $l_v := D_s/v = b_v^{-1}$, $\mathcal{J}_0 := J(0)$, and $\mu_0 := \mu(0)$. By $\mu = -\Omega g_3 \partial_x (|\partial_x h| \partial_x h)$, $g_3 > 0$, we obtain the relation

$$(6.5) \quad \hat{g}_3 (\partial_x h)^2 = (-T + l_v \mathcal{J}_0) x + l_v (\mu_0 + T - l_v \mathcal{J}_0) (e^{x/l_v} - 1) \quad x > 0; \quad \hat{g}_3 = \Omega g_3.$$

The above formula is simplified for $0 < x \ll |l_v|$ (weak drift) and for $x \gg |l_v|$ (strong drift). Accordingly, we obtain the approximation

$$(6.6) \quad |\partial_x h| \sim \hat{g}_3^{-1/2} \begin{cases} \sqrt{\mu_0 x}, & x \ll |l_v|, \\ \sqrt{l_v(\mu_0 + T - l_v \mathcal{J}_0)} e^{x/(2l_v)}, & x \gg l_v > 0, \\ \sqrt{(-|l_v| \mathcal{J}_0 - T)x}, & x \gg -l_v > 0. \end{cases}$$

For $x \gg -l_v > 0$, a compatibility condition is

$$(6.7) \quad -D_s \mathcal{J}_0 > T|v|.$$

By (6.6), changes of the electric-field magnitude and direction can cause a drastic qualitative change in the slope behavior. In particular, a strong electric force Z^*eE in the step-down direction causes an increase of the slope, as steps tend to bunch. (Ultimately, of course, m approaches $\mathcal{O}(\sqrt{x})$ as $x \downarrow 0$.) This behavior is reversed by a strong electric force in the step-up direction, which restores the familiar $\mathcal{O}(\sqrt{x})$ behavior, as this field tends to uniformize the step train.

6.2.2. Axisymmetric structure. The radial case provides a model for the interplay of step edge curvature and electric field. Suppose that the surface is axisymmetric, $h = h(r)$, with the facet $\{(r, h) \in \mathbb{R}_+ \times \mathbb{R} \mid h = \text{const}\}$ in $0 \leq r \leq r_f$ while $\partial_r h < 0$ for $r > r_f$; so, the facet edge is at $r = r_f$. Consider a constant drift velocity v . The ODE for $\mu(r)$ is $\partial_r \mu - l_v^{-1} \mu = l_v^{-1} T - r_f \mathcal{J}_0 / r$, with solution

$$(6.8) \quad \mu = (\mu_0 + T)e^{(r-r_f)/l_v} - T - r_f \mathcal{J}_0 \int_{r_f}^r \frac{e^{(r-r')/l_v}}{r'} dr' \quad r > r_f,$$

where $\mu_0 := \mu(r_f)$, $\mathcal{J}_0 := J(r_f)$. Taking into account that $\Omega^{-1} \mu = g_1/r + g_3 r^{-1} \partial_r [r(\partial_r h)^2]$ where g_1 is the step line tension [26], by direct integration we have

$$(6.9) \quad \hat{g}_3 (\partial_r h)^2 \sim [l_v r_f \mathcal{J}_0 (1 - l_v/r_f) - \hat{g}_1 - r_f T](r - r_f) + (T + \mu_0) l_v [(r - l_v) e^{(r-r_f)/l_v} - r_f + l_v] - l_v (r_f \mathcal{J}_0) (r - l_v) \int_{r_f}^r \frac{e^{(r-r')/l_v}}{r'} dr', \quad 0 < \frac{r - r_f}{r_f} \ll 1;$$

$\hat{g}_l := \Omega g_l$ ($l = 1, 3$). Here, we consider distances $r - r_f$ from the facet boundary that are small compared to the facet radius of curvature. By analogy with section 6.2.1, we simplify the formula for $\partial_r h$ by imposing a relatively weak or strong drift:

$$(6.10) \quad |\partial_r h| \sim \hat{g}_3^{-1/2} \begin{cases} \sqrt{(\mu_0 - \hat{g}_1/r_f)(r - r_f)}, & 0 < r - r_f \ll |l_v|, \\ [l_v(\mu_0 + T - l_v \mathcal{J}_0)]^{1/2} e^{(r-r_f)/(2l_v)}, & r - r_f \gg l_v > 0, \\ \sqrt{(|l_v| |\mathcal{J}_0| - T - \hat{g}_1/r_f)(r - r_f)}, & r - r_f \gg -l_v > 0. \end{cases}$$

The approximation for $r - r_f \gg -l_v > 0$ is compatible with the condition

$$(6.11) \quad -D_s \mathcal{J}_0 > (T + \hat{g}_1/r_f)|v|.$$

Finally, we add a comment on the extension of this analysis to a 2D setting.

Remark 6.3. Approximations analogous to the radial case can be worked out in 2D by use of a local coordinate η normal to the facet boundary, and another coordinate σ parallel to the facet edge. Variations with respect to η are dominant in the vicinity of the facet, in the spirit of variable separation into fast and slow. This approach provides formulas that directly generalize the radial case and is not further discussed here.

7. Conclusion. Starting with the BCF model of step flow, we derived macroscopic evolution laws for the surface height in settings with an electric field. We considered microscopic processes of isotropic as well as anisotropic adatom diffusion on terraces, attachment and detachment of atoms at step edges with an Ehrlich–Schwoebel barrier, diffusion of edge atoms, and desorption of atoms to the surrounding vapor. Energetic effects such as entropic and elastic dipole step interactions were included. We provided a preliminary analysis of how the electric field can affect the surface slope near the edge of a facet with recourse to stationary profiles.

Our central contribution is law (1.2), and its linearized version (1.3) or (4.3), which relate surface flux \mathbf{J} , chemical potential μ , and drift velocity \mathbf{v} . The combination of μ and $\nabla\mu$ of this law is consolidated into a single variable ϑ by exponential transformation (4.22). Accordingly, the PDE for the height is recast to form (4.18), derived previously for isotropic terrace diffusion without an electric field. We showed that desorption is a higher-order effect in the sense of multiscale expansions in the step height. Entertaining, however, the idea of assessing quantitatively the desorption effect, we derived desorption-dependent corrections to the large-scale flux. The nature (and possible value) of these corrections is unclear at the moment.

Many effects are absent from our analysis. For instance, material deposition from above, where the PDE for the height is very different [38, 55], is not considered here. The primary reason for this omission is a subtlety in handling directions normal and parallel to step edges in the limiting procedure. Time-dependent, coupled electromagnetic fields are not accounted for. In the same vein, the *control* of *evolving* surface morphologies by electric fields was barely touched upon. Our assumption of a slowly varying step train restricts the validity of the PDE outside facets and in regions where the steps do not experience drastic instabilities. We also leave out long-range step interactions, e.g., interactions mediated by bulk stress. The issue of boundary conditions for the derived PDE was not addressed. The appropriate boundary conditions must take into account the motion of steps at extrema of a step train [27].

Establishing a connection between the macroscopic theory and experimental data is a largely elusive issue. Addressing this issue requires exhaustive numerical simulations of PDE solutions for a physically admissible and accessible class of initial data. Recent numerics [1] with negligible step line tension (suppressing facets) have demonstrated intriguing relaxation phenomena that beg for quantitative understanding.

Appendix A. Macroscopic limits of 1D step models. In this appendix, we delineate the limits of the adatom flux for the step models of section 2 as $\delta x \equiv \delta x_i = x_{i+1} - x_i \downarrow 0$ (straight steps); or $\delta r \equiv \delta r_i = r_{i+1} - r_i \downarrow 0$ (circular steps).

A.1. Straight steps. Consider $\tau = \infty$. With $vD_s^{-1}\delta x \ll 1$, (2.11) reduces to

$$(A.1) \quad J_i(x_i) \sim -\frac{C_{i+1}^{\text{eq}} - C_i^{\text{eq}} - vD_s^{-1}\delta x C_i^{\text{eq}}}{2k^{-1} + \delta x D_s^{-1}(1 + v/k_u)} \xrightarrow[\delta x \downarrow 0]{v/k_u \ll 1} -D_s \frac{\partial_x C^{\text{eq}} - D_s^{-1}vC^{\text{eq}}}{1 + q|\partial_x h|},$$

which is in agreement with Proposition 4.1; cf. (4.11).

Next, consider $v = 0$ and finite τ . With $b\delta x \ll 1$, (2.14) yields

$$(A.2) \quad J_i(x_i) \sim -D_s \frac{C_{i+1}^{\text{eq}} - C_i^{\text{eq}} - \left(\frac{D_s}{k_d} + \frac{\delta x}{2}\right) b^2 \delta x C_i^{\text{eq}}}{\frac{2D_s}{k} + \delta x + \frac{D_s b}{k_u} \frac{D_s b}{k_d} \delta x + \frac{D_s}{k} (b\delta x)^2} \\ \xrightarrow{\delta x \downarrow 0} -D_s \frac{\partial_x C^{\text{eq}} - (1 + q_d |\partial_x h|) (2D_s \tau)^{-1} \frac{a}{|\partial_x h|} C^{\text{eq}}}{1 + q |\partial_x h| + \frac{D_s}{k_u k_d \tau} + \frac{1}{k \tau} \frac{a}{|\partial_x h|}}; \quad q_d := \frac{2D_s}{k_d a},$$

which is consistent with (5.21) and (5.22). By the conditions $D_s/(k_\ell a) = \mathcal{O}(1)$ and $a \ll k_\ell \tau$ ($\ell = u, d$), the continuum-scale flux (to leading order in a) is

$$(A.3) \quad J(x) = -D_s \frac{\partial_x C^{\text{eq}}}{1 + q |\partial_x h|}.$$

Now take $v \neq 0$ and finite τ via (2.16) and (2.17). Of particular interest are conditions under which the large-scale flux acquires the 1D form of (1.3). For $b_\pm \delta x \ll 1$, $v/D_s \gg (k_\ell \tau)^{-1}$, and $v \ll k_\ell$ ($\ell = u, d$), the denominator $\mathcal{D}_i^{\tau v}$ reduces to

$$(A.4) \quad \mathcal{D}_i^{\tau v} \sim v(b_+ + b_-)(\delta x/D_s + k_d^{-1} + k_u^{-1}),$$

by use of the exact relations $b_+ - b_- = b_v$ and $b_+ b_- = b^2$. Under the same conditions, the numerator in (2.16) acquires the factor $b_+ + b_-$, which is canceled by the factor in (A.4), and the mass flux reduces to (A.1).

A.2. Concentric circular steps. Set $\tau = \infty$ with recourse to (2.35). For $D_s^{-1} v \delta r \ll 1$, we have

$$\phi_i(r) \sim r^{-1} \exp[D_s^{-1} v (r - r_i)] \sim r^{-1} [1 + D_s^{-1} v (r - r_i)], \\ \int_{r_i}^{r_{i+1}} \phi_i(z) dz \sim \ln \frac{r_{i+1}}{r_i} + D_s^{-1} v \left(\delta r - r_i \ln \frac{r_{i+1}}{r_i} \right) \sim \frac{\delta r}{r_i}.$$

Thus, (2.35) reduces to

$$(A.5) \quad J_i(r_i) \sim -D_s \frac{C_{i+1}^{\text{eq}} - C_i^{\text{eq}} + (2v/k) C_i^{\text{eq}}}{2D_s/k + (1 + v/k_u) \delta r} + v \frac{D_s(k_u^{-1} C_{i+1}^{\text{eq}} + k_d^{-1} C_i^{\text{eq}}) + \delta r C_i^{\text{eq}}}{2D_s/k + (1 + v/k_u) \delta r} \\ \xrightarrow{\frac{v/k_u \ll 1}{\delta r \downarrow 0}} -D_s (1 + q |\partial_r h|)^{-1} (\partial_r C^{\text{eq}} - D_s^{-1} v C^{\text{eq}}),$$

in agreement with Proposition 4.1; cf. (4.11).

Appendix B. Alternate proof of Proposition 4.1. In this appendix, we rely on Taylor expansions avoiding use of integration constants to prove Proposition 4.1. In the limit $\delta \eta_i \downarrow 0$, we expand in Taylor series about (η_i, σ) the adatom concentration and normal flux that appear in the step-down boundary condition (3.5) for $\sigma' = \sigma$:

$$(B.1) \quad C_i(\eta_{i+1}) = C_i(\eta_i) + \delta \eta_i \partial_\eta C_i(\eta_i) + \mathcal{O}(\delta \eta_i^2),$$

$$(B.2) \quad J_{i,\perp}(\eta_{i+1}) = J_{i,\perp}(\eta_i) + \delta \eta_i \partial_\eta J_{i,\perp}(\eta_i) + \mathcal{O}(\delta \eta_i^2).$$

To express the η -derivatives in terms of C_i and $J_{i,\perp}$, we use Fick's law (3.3) and its η -derivative, along with the diffusion equation (3.2), rewritten here for convenience:

$$(B.3) \quad \xi_\eta^{-1} \partial_\eta C_i = -D_s^{-1} (J_{i,\perp} - v_\perp C_i),$$

$$(B.4) \quad \partial_\eta J_{i,\perp} \sim -D_s \xi_\eta^{-1} \partial_\eta^2 C_i + v_\perp \partial_\eta C_i, \quad \partial_\eta \xi_\eta, \partial_\eta v_\perp = o(1),$$

$$(B.5) \quad \partial_\eta^2 C_i = -(\partial_\eta C_i) \left(-\frac{\xi_\eta v_\perp}{D_s} + \partial_\eta \ln \frac{\xi_\sigma}{\xi_\eta} \right).$$

Substitution of (B.1) and (B.2) into the step-down boundary condition (3.5) yields

$$(B.6) \quad C_{i+1}^{\text{eq}} = C_i(\eta_i) \left[1 + \frac{v_\perp \xi_\eta \delta \eta_i}{D_s} \left(1 - \frac{v_\perp}{k_d} \right) - \frac{v_\perp \delta \eta_i}{k_d} \left(-\frac{\xi_\eta v_\perp}{D_s} + \partial_\eta \ln \frac{\xi_\sigma}{\xi_\eta} \right) \right] \\ + J_{i,\perp}(\eta_i) \left[-\frac{1}{k_d} - \frac{\xi_\eta \delta \eta_i}{D_s} \left(1 - \frac{v_\perp}{k_d} \right) + \frac{\delta \eta_i}{k_d} \left(-\frac{\xi_\eta v_\perp}{D_s} + \partial_\eta \ln \frac{\xi_\sigma}{\xi_\eta} \right) \right].$$

By accounting for the step-up boundary condition (3.4), we have

$$(B.7) \quad \begin{pmatrix} C_i^{\text{eq}} \\ C_{i+1}^{\text{eq}} \end{pmatrix} = \begin{pmatrix} 1 & 1 + \frac{v_\perp \xi_\eta \delta \eta_i}{D_s} \left(1 - \frac{v_\perp}{k_d} \right) - \frac{v_\perp \delta \eta_i}{k_d} \left(-\frac{\xi_\eta v_\perp}{D_s} + \partial_\eta \ln \frac{\xi_\sigma}{\xi_\eta} \right) \\ \frac{1}{k_u} & -\frac{1}{k_d} - \frac{\xi_\eta \delta \eta_i}{D_s} \left(1 - \frac{v_\perp}{k_d} \right) + \frac{\delta \eta_i}{k_d} \left(-\frac{\xi_\eta v_\perp}{D_s} + \partial_\eta \ln \frac{\xi_\sigma}{\xi_\eta} \right) \end{pmatrix}^T \cdot \begin{pmatrix} C_i \\ J_{i,\perp} \end{pmatrix},$$

where the variables on the right-hand side are evaluated at (η_i, σ) . Left-multiply (B.7) by the elimination matrix

$$\begin{pmatrix} 1 & 0 \\ -1 - \frac{v_\perp \xi_\eta \delta \eta_i}{D_s} + \frac{v_\perp \delta \eta_i}{k_d} \partial_\eta \ln \frac{\xi_\sigma}{\xi_\eta} & 1 \end{pmatrix}$$

to obtain an equation for the normal flux component:

$$(B.8) \quad J_{i,\perp} \left[\frac{1}{k_u} + \frac{1}{k_d} + \frac{\xi_\eta \delta \eta_i}{D_s} \left(1 + \frac{v_\perp}{k_u} \right) \left(1 - \frac{D_s}{k_d \xi_\sigma} \partial_\eta \frac{\xi_\sigma}{\xi_\eta} \right) \right] = C_i^{\text{eq}} - C_{i+1}^{\text{eq}} \\ + \frac{v_\perp \xi_\eta \delta \eta_i}{D_s} \left(1 - \frac{D_s}{k_d \xi_\sigma} \partial_\eta \ln \frac{\xi_\sigma}{\xi_\eta} \right) C_i^{\text{eq}}.$$

In the limit $\delta \eta_i \downarrow 0$, (B.8) approaches

$$(B.9) \quad J_{i,\perp} \left(1 + 2 \frac{D_s}{k_d} |\nabla h| \right) = -D_s C_s \left[\frac{\nabla \mu}{T} - \frac{v_\perp}{D_s} \left(1 + \frac{\mu}{T} \right) \right],$$

which we identify with the first (η -) component of (4.3). The σ -component of the flux follows by differentiating with respect to σ the solution for C_i from (B.7).

Acknowledgments. We are indebted to John D. Weeks for valuable discussions. We wish to thank Andrea Bonito and Ricardo H. Nochetto for discussing with us details of the finite element method; and Matthieu Dufay, Theodore L. Einstein, Ray Phaneuf, and Ellen D. Williams for useful conversations. The first author (J. Quah) acknowledges the generous support of a Monroe Martin Graduate Fellowship at the University of Maryland during the summer of 2008, when part of this work was completed. The second author (D. Margetis) appreciates the support of the Maryland NanoCenter.

REFERENCES

- [1] A. BONITO, R. H. NOCHETTO, J. QUAH, AND D. MARGETIS, *Self-organization of decaying surface corrugations: A numerical study*, Phys. Rev. E, 79 (2009), 050601.
- [2] W. K. BURTON, N. CABRERA, AND F. C. FRANK, *The growth of crystals and the equilibrium structure of their surfaces*, Philos. Trans. R. Soc. Lond. Ser. A, 243 (1951), pp. 299–358.
- [3] J. CHANG, O. PIERRE-LOUIS, AND C. MISBAH, *Birth and morphological evolution of step bunches under electromigration*, Phys. Rev. Lett., 96 (2006), 195901.
- [4] M. DUFAY, T. FRISCH, AND J.-M. DEBIERRE, *Role of step-flow advection during electromigration-induced step bunching*, Phys. Rev. B, 75 (2007), 241304.
- [5] W. E AND N. K. YIP, *Continuum theory of epitaxial growth. I*, J. Stat. Phys., 104 (2001), pp. 221–253.
- [6] G. EHRLICH AND F. HUDDA, *Atomic view of surface diffusion: Tungsten on tungsten*, J. Chem. Phys., 44 (1966), pp. 1039–1099.
- [7] A. ERDÉLYI, ED., *Bateman Manuscript Project: Higher Transcendental Functions, Vol. I*, Krieger, Malabar, FL, 1981.
- [8] J. W. EVANS, P. A. THIEL, AND M. C. BARTELT, *Morphological evolution during epitaxial thin film growth: Formation of 2D islands and 3D mounds*, Surf. Sci. Rep., 61 (2006), pp. 1–128.
- [9] L. C. EVANS, *Partial Differential Equations*, AMS, Providence, RI, 1998.
- [10] P.-W. FOK, *Simulation of Axisymmetric Stepped Surfaces with a Facet*, Ph.D. thesis, Massachusetts Institute of Technology, Cambridge, MA, 2006.
- [11] P.-W. FOK, R. ROSALES, AND D. MARGETIS, *Unification of step bunching phenomena on vicinal surfaces*, Phys. Rev. B, 76 (2007), 033408.
- [12] T. FRISCH AND A. VERGA, *Kinetic step bunching instability during surface growth*, Phys. Rev. Lett., 94 (2005), 226102.
- [13] E. S. FU, D.-J. LIU, M. D. JOHNSON, J. D. WEEKS, AND E. D. WILLIAMS, *The effective charge in surface electromigration*, Surf. Sci., 385 (1997), pp. 259–269.
- [14] P. S. HO AND T. KWOK, *Electromigration in metals*, Rep. Progr. Phys., 52 (1989), pp. 301–348.
- [15] N. ISRAELI AND D. KANDEL, *Profile of a decaying crystalline cone*, Phys. Rev. B, 60 (1999), pp. 5946–5962.
- [16] H.-C. JEONG AND E. D. WILLIAMS, *Steps on surfaces: Experiments and theory*, Surf. Sci. Rep., 34 (1999), pp. 171–294.
- [17] J. KRUG, *Introduction to step dynamics and step instabilities*, in Multiscale Modeling of Epitaxial Growth, International Series of Numerical Mathematics 149, A. Voigt, ed., Birkhäuser, Basel, 2005, pp. 69–95.
- [18] J. KRUG, *Nonlinear dynamics of surface steps*, 2008, preprint, cond-math.mtrl-sci/arXiv:0810.5749.
- [19] J. KRUG, V. TONCHEV, S. STOYANOV, AND A. PIMPINELLI, *Scaling properties of step bunches induced by sublimation and related mechanisms*, Phys. Rev. B, 71 (2005), 045412.
- [20] A. V. LATYSHEV, A. L. ASEEV, A. B. KRASILNIKOV, AND S. I. STENIN, *Transformations on clean Si(111) stepped surface during sublimation*, Surf. Sci., 213 (1989), pp. 157–169.
- [21] D.-J. LIU AND J. D. WEEKS, *Quantitative theory of current-induced step bunching on Si(111)*, Phys. Rev. B, 57 (1998), pp. 14891–14900.
- [22] D.-J. LIU, J. D. WEEKS, AND D. KANDEL, *Current-induced step bending instability on vicinal surfaces*, Phys. Rev. Lett., 81 (1998), pp. 2743–2746.
- [23] V. I. MARCHENKO AND A. YA. PARSHIN, *Elastic properties of crystal surfaces*, Sov. Phys. JETP, 52 (1980), pp. 129–131.
- [24] D. MARGETIS, *Notions of Crystal Surface Composites: Prelude to Self-Organization*, manuscript.
- [25] D. MARGETIS, *Unified continuum approach to crystal surface morphological relaxation*, Phys. Rev. B, 76 (2007), 193403.
- [26] D. MARGETIS, M. J. AZIZ, AND H. STONE, *Continuum approach to self-similarity and scaling in continuum relaxation of a crystal with a facet*, Phys. Rev. B, 71 (2005), 165432.
- [27] D. MARGETIS, P.-W. FOK, M. J. AZIZ, AND H. A. STONE, *Continuum theory of nanostructure decay via a microscale condition*, Phys. Rev. Lett., 97 (2006), 096102.
- [28] D. MARGETIS AND R. V. KOHN, *Continuum theory of interacting steps on crystal surfaces in 2 + 1 dimensions*, Multiscale Model. Simul., 5 (2006), pp. 729–758.
- [29] J. J. MÉTOIS, J. C. HEYRAUD, AND S. STOYANOV, *Step flow growth of vicinal (111) Si surface at high temperatures: Step kinetics or surface diffusion control*, Surf. Sci., 486 (2001), pp. 95–102.

- [30] T. MICHELY AND J. KRUG, *Islands, Mounds and Atoms: Patterns and Processes in Crystal Growth Far From Equilibrium*, Springer-Verlag, Berlin, 2004.
- [31] C. MISBAH AND O. PIERRE-LOUIS, *Pulses and disorder in a continuum version of step-bunching dynamics*, Phys. Rev. E, 53 (1996), pp. R4318–R4321.
- [32] P. NOZIÈRES, *On the motion of steps on a vicinal surface*, J. Phys. (France), 48 (1987), pp. 1605–1608.
- [33] M. OZDEMIR AND A. ZANGWILL, *Morphological equilibration of a corrugated crystalline surface*, Phys. Rev. B, 42 (1990), pp. 5013–5024.
- [34] O. PIERRE-LOUIS, *Step bunching with general step kinetics: Stability analysis and macroscopic models*, Surf. Sci., 529 (2003), pp. 114–134.
- [35] O. PIERRE-LOUIS, *Dynamics of crystal steps*, C. R. Phys., 6 (2005), pp. 11–21.
- [36] O. PIERRE-LOUIS, *Local electromigration model for crystal surfaces*, Phys. Rev. Lett., 96 (2006), 135901.
- [37] O. PIERRE-LOUIS AND J.-J. MÉTOIS, *Kinetic step pairing*, Phys. Rev. Lett., 93 (2004), 165901.
- [38] P. POLITI AND J. VILLAIN, *Ehrlich-Schwoebel instability in molecular-beam epitaxy: A minimal model*, Phys. Rev. B, 54 (1996), pp. 5114–5129.
- [39] J. QUAH AND D. MARGETIS, *Anisotropic diffusion in continuum relaxation of stepped crystal surfaces*, J. Phys. A: Math. Theor., 41 (2008), 235004.
- [40] J. QUAH, J. YOUNG, AND D. MARGETIS, *Macroscopic view of crystal-step transparency*, Phys. Rev. E, 78 (2008), 042602.
- [41] A. RETTORI AND J. VILLAIN, *Flattening of grooves on a crystal surface: A method of investigation of surface roughness*, J. Phys. (France), 49 (1988), pp. 257–267.
- [42] M. SATO, M. UWAHA, AND Y. SAITO, *Evaporation and impingement effects on drift-induced step instabilities on a Si(001) vicinal surface*, Phys. Rev. B, 72 (2005), 045401.
- [43] M. SATO, M. UWAHA, Y. SAITO, AND Y. HIROSE, *Step wandering induced by the drift of adatoms in a conserved system*, Phys. Rev. B, 65 (2002), 245427.
- [44] M. SCHIMSCHAK AND J. KRUG, *Surface electromigration as a moving boundary value problem*, Phys. Rev. Lett., 78 (1997), pp. 278–281.
- [45] R. L. SCHWOEBEL AND E. J. SHIPSEY, *Step motion on crystal surfaces*, J. Appl. Phys., 37 (1966), pp. 3682–3686.
- [46] V. B. SHENOY AND L. B. FREUND, *A continuum description of the energetics and evolution of stepped surfaces in strained nanostructures*, J. Mech. Phys. Solids, 50 (2002), pp. 1817–1841.
- [47] H. SPOHN, *Surface dynamics below the roughening transition*, J. Phys. I (France), 3 (1993), pp. 69–81.
- [48] J. STANGL, V. HOLÝ, AND G. BAUER, *Structural properties of self-organized semiconductor nanostructures*, Rev. Mod. Phys., 76 (2004), pp. 725–783.
- [49] S. STOYANOV, *Electromigration induced step bunching on Si surfaces—How does it depend on temperature and heating current direction?*, Japan J. Appl. Phys., 30 (1991), pp. 1–6.
- [50] S. STOYANOV, *Scaling properties of step bunches formed on vicinal crystal surfaces during MBE growth*, Surf. Sci., 464 (2000), pp. L715–L718.
- [51] S. STOYANOV AND V. TONCHEV, *Properties and dynamic interaction of step density waves at a crystal surface during electromigration affected sublimation*, Phys. Rev. B, 58 (1998), pp. 1590–1600.
- [52] I. N. STRANSKI, *Zur theorie des kristallwachstums*, Z. Chem., 136 (1928), pp. 259–278.
- [53] F. G. TRICOMI, *Integral Equations*, Dover, New York, 1985.
- [54] D. D. VVEDENSKY, *Multiscale modelling of nanostructures*, J. Phys.: Condens. Matter, 16 (2004), pp. R1537–R1576.
- [55] J. VILLAIN, *Continuum models of crystal growth from atomic beams with and without desorption*, J. Phys. I, 1 (1991), pp. 19–42.
- [56] Y. XIANG, *Derivation of a continuum model for epitaxial growth with elasticity on vicinal surface*, SIAM J. Appl. Math., 63 (2002), pp. 241–258.
- [57] T. ZHAO, J. D. WEEKS, AND D. KANDEL, *Unified treatment of current-induced instabilities on Si surfaces*, Phys. Rev. B, 70 (2004), 161303(R).
- [58] T. ZHAO, J. D. WEEKS, AND D. KANDEL, *From discrete hopping to continuum modeling on vicinal surfaces with applications to Si(001) electromigration*, Phys. Rev. B, 71 (2005), 155326.